*Russian Chemical Reviews* **76** (5) 435 – 461 (2007) © 2007 Russian Academy of Sciences and Turpion Ltd

DOI 10.1070/RC2007v076n05ABEH003674

# Nanotechnologies. Properties and applications of nanostructured materials

A A Rempel

## Contents


| | | |
|---|---|---|
| I. | Introduction | 435 |
| II. | Vapour condensation and gas-phase synthesis | 436 |
| III. | Plasmochemical synthesis | 437 |
| IV. | Deposition from colloidal solutions | 439 |
| V. | Pyrolysis | 443 |
| VI. | Mechanosynthesis | 443 |
| VII. | Detonation-induced synthesis | 446 |
| VIII. | Self-propagating high-temperature synthesis | 446 |
| IX. | Compaction of nanopowders | 446 |
| X. | Crystallisation of amorphous alloys | 448 |
| XI. | Severe plastic deformation | 448 |
| XII. | Electric explosion | 450 |
| XIII. | Ordering of non-stoichiometric compounds as a method for the construction of nanostructures | 450 |
| XIV. | Properties and application of nanomaterials | 453 |
| XV. | Conclusion | 456 |


**Abstract. The review summarises the main methods for the preparation of nanostructured metals, alloys, semiconductors and ceramics. The formation mechanisms of nanostructures based on two different principles, *viz*. the assembly principle (bottom-up) and the disintegration principle (top-down), are analysed. Isolated nanoparticles, nanopowders and compact nanomaterials produced by these methods possess different properties. The scope of application of various classes of nanostructured materials is considered and the topicality of the development of nanoindustry is emphasised. The bibliography includes 271 references.**

## I. Introduction

A large body of the available experimental data on nanomaterials and nanotechnologies provided the basis for the generalisation of fundamental and applied results in reviews and monographs.[1 – 20]

Due to the development of the nanoscience in recent years, the data on nanotechnologies and nanomaterials become more abundant and new, sometimes unexpected, properties are revealed. Hence, the present review begins with the author's point of view on the nomenclature and comparative characterisation of the concept of nanomaterials and other similar (often related) notions.

**A A Rempel** Institute of Solid State Chemistry, Urals Branch of the Russian Academy of Sciences, ul. Pervomaiskaya 91, 620041 Ekaterinburg, Russian Federation. Fax (7-343) 374 44 95, tel. (7-343) 374 73 06, e-mail: rempel@ihim.uran.ru

Received 25 October 2006
*Uspekhi Khimii* **76** (5) 474 – 500 (2007); translated by T N Safonova

The term nanotechnology refers to the methods used for the construction of nanomaterials and nanodevices and methods of handling of nanoobjects. Nanotechnologies produce nanometre-size particles. These technologies are based on methods allowing the construction of objects with sizes that are thousand or even million times smaller than those visible to the human eye. The systematic and purposeful development of the fundamentals of nanotechnologies started several decades ago. Nowadays, the results of investigations in this field are introduced in industry. In the present review, emphasis is given to procedures for the preparation of nanostructured materials, their properties and promising fields of application.

Nanotechnologies aimed at preparing nanostructured materials can arbitrarily be divided into the following two groups: bottom-up and top-down. This classification takes into account the key step (or the process) of nanotechnology where a nanostructure is formed. The former group includes methods, in which nanoparticles are formed from atoms and molecules, *i.e.*, the starting species are enlarged to nanometre sizes; the latter group, methods in which nanometre sizes are achieved by disintegration of larger particles, powders or grains. The former group of methods of nanotechnology are based primarily on the chemical approach, while the latter group of methods, on the physical approach. In many cases, nanomaterials with the same chemical composition but with different properties can be prepared using these two different in principle groups of technologies.

A decrease in the particle size of a solid below a certain threshold leads to a considerable change in its properties. For most known materials, the threshold at which a jumpwise change in the properties occurs (the so-called size effect) varies from 1 to 100 nm.

Of course, all materials composed of nanometre-size building blocks can be referred to as nanomaterials. Large molecules, clusters, material particles or polycrystalline grains can

serve as building blocks. However, in this case, the term 'nanomaterial' would be narrowed to the simple statement of the block size, and it would be unclear why the development of nanotechnologies is considered as a new technology revolution. Hence, it is necessary that the concept of a nanomaterial include not only the size of building blocks, but also a jumpwise change in properties of materials that occurs as the nanometre size is achieved.

In some publications, the term nanomaterials refers to highly dispersed, ultrafine-grain, superfine-grain or ultrathin materials. This is unjustified because the concept of nanomaterials includes a quantitative parameter, *viz*., the size of a particle, grain or building block, reflected in the prefix 'nano'. In the other above-mentioned systems, the building block size is reflected only qualitatively (a small or supersmall size without mentioning its particular value), *i.e*., the sizes are uncertain and relative. Consequently, the use of the term nanomaterials in relation to these systems should be avoided wherever possible.

The concept of nanomaterials should not be also confused with another commonly accepted concept of submicrocrystalline materials. The properties of submicrocrystalline materials, like those of nanomaterials, differ from the properties of coarsely crystalline, coarse-grain and single-crystalline materials. However, the difference in the properties is associated primarily with increased specific surface area which results in acceleration of various processes, *e.g*., chemical reactions, but does not lead to a decrease in the activation energy (*i.e*., to a decrease in the temperature of the beginning of the reaction). In submicrocrystalline materials, the particle, grain or building block size is assumed to be smaller than a micrometre. A micrometre, like a nanometre, is a quantitative characteristic. However, there is a difference in principle between nanomaterials and submicrocrystalline materials. It is the nanostate rather than the submicrocrystalline state that is intermediate between the molecular and solid states. The properties of solids are manifested at nanometre distances. This is also the physical reason of substantial changes in the properties observed on the nanometre-size scale. The fact is that the lengths at which the main physical forces act in materials vary from 1 to 100 nm. It should be noted that different types of interactions, *viz*., electron–electron, electron–phonon, phonon–phonon, magnon–magnon, *etc*., are extended to different distances in the same material. Hence these interactions can be observed for different nanoparticle sizes. It is evident that the nanoparticle size is of no fundamental importance for the same or different materials.

Nanomaterials are often called nanocrystalline materials. This is also not always justified. Crystalline particles or grains serve as building blocks in nanocrystalline materials. However, nanomaterials are, as a rule, thermodynamically non-equilibrium systems and, consequently, their building blocks do not necessarily have perfect crystal structures.[21] It is more likely that the situation is opposite. Building blocks in nanomaterials often have highly defective structures. Sometimes, their state is close to amorphous. In other words, the long-range order in building blocks of nanomaterials can be violated, and multiparticle correlations in the atom arrangement are determined by the short-range order. Hence, the more correct and complete name for nanomaterials should be 'nanostructured materials'.

Different classifications of nanomaterials are associated with their diversity. The most appropriate classification is based on the size of building blocks or their constituent structural elements. The main types of nanomaterials are zero- (0D), one- (1D), two- (2D) and three-dimensional (3D). Nanocluster materials and nanodispersions composed of isolated nanoparticles belong to a zero-dimensional type; nanofibre (nanorod) and nanotubular materials, to a one-dimensional type, the fibre (rod) or tube length varying from 100 nm to tens of micrometres. Nanometre-thick films belong to two-dimensional nanomaterials. Nanoparticles in 0D, 1D and 2D nanomaterials are often embedded in a liquid or solid matrix or are deposited onto a support. Powders, fibre, multilayer and polycrystalline materials, in which 0D, 1D and 2D particles are closely packed together to form interfaces, belong to three-dimensional nanomaterials. A polycrystal containing nanometre-size grains is an example of three-dimensional nanomaterials. In such polycrystals, the total bulk is occupied by nanograins, the free surface of grains is virtually absent, and only grain interfaces are present. The formation of interfaces and the 'disappearance' of the nanoparticle surface in three-dimensional nanomaterials is of fundamental importance for the understanding of the nature of their properties. Actually, the properties of a strongly agglomerated nanopowder can be substantially different from those of a compact nanomaterial consisting of particles of the same size as the powder. In the last two decades, considerable attention was given to the preparation of 3D nanomaterials. It is three-dimensional nanomaterials that will be used in the hard-alloy production, the aircraft construction and hydrogen power engineering in the nearest future.

Nowadays, a rather wide range of nanomaterials is available.[11–20] In the present review, methods for the preparation of dense three-dimensional and two-dimensional nanostructured materials are considered.

## II. Vapour condensation and gas-phase synthesis

One of the simplest procedures for the preparation of nanoparticles is based on vapour condensation in an inert atmosphere under reduced pressure. This method can be applied to the preparation of nanoparticles of both simple and complex compounds. Synthesis of nanoparticles of metal compounds, for example, of oxides, nitrides, carbides, *etc*., requires that the corresponding reaction gas (oxygen, nitrogen, carbon dioxide, methane, *etc*.) be added. The simplest way to a material vapour is evaporation. The atoms of vaporised substances rapidly lose the kinetic energy and form nanoparticles. In the case of metal compounds, the metal atoms react with the reaction gas. Particles of the desired size can be formed by adjusting the inert gas pressure. The formation of nanoparticles according to this method was systematically studied for Zn, Cd, Se, As and Au. Particles with sizes from 2 to 100 nm were prepared,[22–24] the optimum inert gas pressure being in the range from 40 to 400 Pa.

It is difficult to collect nanoparticles formed upon condensation because nanoparticles are not deposited under the force of gravity but exist in the suspended state in the Brownian motion. Nanoparticles are usually collected on a cold surface or on filters.

Nanoparticles can also be prepared by dispersing a metal in a liquid with the use of an electric arc followed by condensation of a metal vapour in a liquid vapour.[25] The features of condensation in a supersaturated vapour, which proceeds through the nucleation and nucleus growth, were considered in the reviews.[26–28]

The shapes of nanoparticles prepared by the gas-phase method depend on their size. Nanoparticles with size $< 20$ nm are spherical in shape due to a change in the relative contribution of the surface energy to the total energy of nanoparticles as their sizes decrease. Larger particles are faceted. Yet another interesting fact associated with the small size of isolated nanocrystals and related to the energy is the absence of dislocations, which are energetically less favourable than disclinations.[29]

In the gas-phase synthesis, nanoparticles are formed upon cooling of a vapour–gas mixture containing one, two or more chemical elements along with an inert gas. Cooling occurs in the condensation zone the size of which in a particular reaction vessel can be controlled by varying the inert gas pressure. The condensation zone increases with a decrease in pressure and *vice versa*. The influence of the change in the inert gas pressure on the resulting nanoparticle size is manifested both directly and through the condensation zone size. An increase in the gas pressure leads to an increase in density, acceleration of heat removal, a decrease in the formation rate of crystallisation centres in the gas phase, but an increase in the growth rate of crystals and, consequently, the resulting particle size. In the gas-phase synthesis of rather small particles (20–30 nm), the inert gas (usually, helium) pressure is maintained at 40–60 Pa.

Preparation of nanoparticles of metal compounds requires that a reaction gas be added to the inert gas medium. Single-crystalline nanoparticles of metal compounds with different morphologies are formed in these reactions. The particle shape can be controlled by varying the composition of the gas phase. For example, CdS can be prepared as prismatic plates, ribbons, needles, whiskers, threads or tubes upon variation of the temperature and deviation of the Cd : S ratio in the gas phase from the stoichiometric ratio (1 : 1) toward an increase in the cadmium content.[30,31] The intermediate clusters $[CdS]_n$, $[Cd_2S]_n$ and $[Cd_3S]_n$ serve as the structural basis of the growth of crystals of different shapes. Thus, the ratio of the starting components of the gas phase and the temperature are the main factors determining the particle shape, whereas their size more strongly depends on the inert gas pressure.

Monodisperse nanoparticles with size $<2$ nm can be prepared by mass separation of clusters in a mass spectrometer. For example, metal vapour is passed through a cell filled with helium under a pressure of $\sim$1000–1500 Pa and then introduced into a vacuum chamber ($\sim 10^{-5}$ Pa). The mass of clusters is determined from the flight time by a particular distance in the mass spectrometer. This method was used for the preparation of antimony, bismuth and lead clusters containing 650, 270 and 400 atoms, respectively. The helium gas temperature in the case of Sb and Bi vapour was 80 K; in the case of a Pb vapour, 280 K.[32]

Diamond nanoparticles can be synthesised from a gas phase supersaturated with respect to carbon ($CO_2$, methane, acetylene, propane and other hydrocarbons) under a subatmospheric pressure.[33,34] Condensation of carbon from the gas phase and diamond nucleation are favoured by an excess surface energy at the solis–gas interface. Deposition of diamond nanoparticles is widely used for the construction of diamond and diamond-containing films and coatings.[35]

Nanocrystalline powders of oxides $Al_2O_3$, $ZrO_2$ and $Y_2O_3$ were prepared by evaporation of oxide targets in a atmosphere helium,[36] magnetron sputtering of zirconium in a mixture of argon and oxygen[37] and controlled oxidation of yttrium nanocrystals.[38] Highly dispersed powders of transition metal nitrides can be synthesised by electron-beam heating of the corresponding metal targets, evaporation being performed in an atmosphere of nitrogen or ammonia at a pressure of 130 Pa.[39]

Metal carbide, oxide and nitride nanoparticles can be synthesised by pulsed laser heating of metals in an atmosphere of methane (for carbides), oxygen (for oxides), nitrogen or ammonia (for nitrides) under reduced pressure.[40] Pulsed laser evaporation of metals in an atmosphere of an inert gas (He or Ar) and reaction gases ($O_2$, $N_2$, $NH_3$ and $CH_4$) affords mixtures of nanocrystalline metal oxides and oxide–nitride and carbide–nitride mixtures. The composition and size of nanoparticles in these mixtures can be controlled by varying the pressure, the composition of the atmosphere, the laser pulse power and the temperature gradient between the evaporated target and the surface onto which condensation occurs.

Nanoparticles of Fe–Ni, Fe–Mn, Fe–Cr, Fe–Pt and Fe–Co iron-rich alloys are prepared under argon at a pressure of 400 Pa.[41] Deposited particles are spherical in shape. Their average size is $25 \pm 5$ nm. As a rule, nanoparticles are two-phase (with bcc or hcc lattices), which corresponds to the thermodynamic equilibrium between the components in these alloys.

An yttrium oxide-doped zirconium oxide film with an average crystallite size of 10–30 nm was prepared by pulsed laser evaporation of metals in an oxygen ion beam followed by deposition of oxides onto a support at 350–700 K.[42]

Nanopowders of ceramic materials can be prepared from organometallic and organoelement compounds. For example, nanocrystalline $SiC_xN_y$ powders were prepared as follows. The starting compound (hexamethyldisilazane) was mixed with an inert carrier gas in a heated tubular reactor serving as an evaporator. Its thermal decomposition affords a continuous cluster or nanoparticle flow, which escapes from the reactor into a working chamber and is condensed in a refrigerator constructed as a rotating cylinder. Nanopowders of $SiO_2$, SiC and $Si_3N_4$ can be synthesised by adding water, hydrogen or ammonia, respectively, along with the same precursor to the carrier gas. The success of the reaction is provided by a low concentration of the organoelement compound in the inert gas, fast expansion and cooling of the gas flow at the exit from the reactor into the working chamber and a low pressure in the working chamber.[43]

## III. Plasmochemical synthesis

The plasmochemical synthesis is most commonly used for the synthesis of highly dispersed boride, carbide, nitride and oxide powders. This method makes use of low-temperature (4000–10 000 K) nitrogen, ammonia, hydrogen, hydrocarbon or argon plasmas produced by arc, glow, high-frequency and superhigh-frequency discharges. The characteristics of the resulting powders depend on the nature of the starting material, the technology and the reactor type. Particles of such powders are most often prepared as single crystals with sizes from 10 to 100–200 nm and larger. For nanoparticles to be synthesised by this method, the reaction should be far from equilibrium and the rate of solid-phase nucleation should be high, whereas the rate of nucleus growth should be low. The plasmochemical synthesis provides high formation and condensation rates of compounds and sufficiently high output. Broad particle size distribution (*i.e.*, low selectivity of the process) and heavy contamination of the powder are the main drawbacks of this method. Highly dispersed powders of titanium, zirconium, hafnium, vanadium, niobium, tantalum, boron, aluminium and silicon nitrides, titanium, niobium, tantalum, tungsten, boron and silicon carbides and magnesium, yttrium and aluminium oxides were prepared by the plasmochemical method.[32,36–51]

At high plasma temperature, all starting compounds pass into the ionised gas state due to which the reaction rates are high and the reaction times are short ($10^{-3}$–$10^{-6}$ s). Active particles are formed in arc, high-frequency and superhigh-frequency plasma reactors. Arc plasma reactors are characterised by the highest power and efficiency; however, materials prepared in such reactors are contaminated by electrode erosion products. Electrodeless high-frequency and plasma ultrasonic reactors are free from this drawback. In the next step, quenching results in the isolation of the reaction products. Powders with the desired composition and with a particular particle shape and size can be prepared by varying the quenching region and rate.

Since nanoparticles synthesised by the plasmochemical method have a large excess energy, their chemical and phase compositions can be inconsistent with the equilibrium phase diagram. Additional short-term annealing of the product in a controlled atmosphere helps in preparing nanoparticles of the required stoichiometry. For example, a tungsten carbide powder was synthesised by the plasmochemical method from tungsten oxide ($WO_3$) and methane in a low-temperature ($\sim 4000-5000$ K) hydrogen plasma flow.[52] A nanocrystalline powder with an average particle size of 20–40 nm was obtained. An X-ray powder diffraction study (Fig. 1 *a*) showed that the powder contained two carbide phases, *viz*., $W_2C$ (>75 mass %) and WC (~5 mass %), and tungsten (~18 mass %). Chemical analysis revealed the presence of free carbon in the powder. To achieve the single-phase state, the synthesised powder was additionally annealed under argon at 800–1000 K. The annealed powder contained only hexagonal (space group *P6m*2) tungsten carbide (Fig. 1 *b*). The size of coherent scattering regions in the annealed powder remained virtually unchanged compared to that in the starting powder, but the particle size determined by scanning electron microscopy [53] increased to 60–120 nm. This suggests agglomeration of nanoparticles in the annealed powder. The retention of the nanoparticle size of WC in the powder after annealing at 800–1000 K is associated with high thermal stability of this compound, as was demonstrated by magnetic susceptibility measurements.[53]

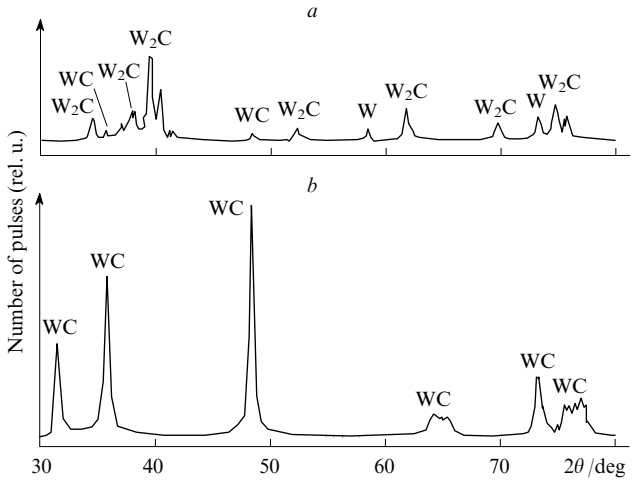



**Figure 1.** X-Ray powder diffraction patterns of tungsten carbide powders prepared directly by the plasmochemical synthesis (*a*) and after additional homogenising annealing (*b*).[52]
The resulting powder is multiphase; after additional annealing under argon, a single-phase powder was obtained; the average nanoparticle size of the powder was 20–40 nm.

The gas-phase synthesis involving laser heating of a reaction mixture is a version of the plasmochemical synthesis.[54, 55] This method is highly competitive with other methods due to its reliability and high efficiency. Laser heating excludes contamination of the reaction mixture and allows the control over homogeneous nucleation. Other advantages of laser heating are that surfaces inducing heterogeneous nucleation are absent and the process can be controlled. A laser is a source of high-intensity monochromatic radiation due to which a high degree of its conversion to heat is achieved. The laser-induced synthesis of nanocrystalline Si, $Si_3N_4$ and SiC powders was described in detail.[54] Silicon powders were prepared by pyrolysis of gaseous silane ($SiH_4$) using a $CO_2$ laser. Silicon grains were spherical in shape with a diameter of $50 \pm 20$ nm and consisted of several crystallites with the size of ~15 nm. Silicon nitride powders were synthesised from a gas mixture of silane and ammonia. The resulting powder was amorphous, and the grains were spherical with a diameter of $17 \pm 4$ nm, the size distribution of grains being narrower than that in a silicon powder (for $Si_3N_4$, the size distribution of grains varied from 10 to 25 nm). Unlike silicon nanoparticles, $Si_3N_4$ grains had no internal structure. Silicon carbide was synthesised from gas mixtures of silane with methane or ethylene. The grain size in the resulting crystalline SiC powder varied from 18 to 26 nm; the average size was 21 nm. The nanoparticle size was demonstrated [54] to decrease as the intensity of the laser radiation increased due to an increase in the temperature and the heating rate of the reagent gases. Grains of nanopowders synthesised by laser heating are characterised by a narrow size distribution and a spherical shape.

The plasmochemical gas-phase synthesis with the use of laser radiation for the plasma production and maintenance proved to be efficient for the preparation of molecular clusters. The latter have polymorphic cage atomic structures and occupy special place among nanoparticles. Fullerenes, which are allotropes of nanocarbon and differ from the known carbon modifications (graphite and diamond), have received most attention.[56–58]

Fullerenes can be synthesised by sputtering of graphite in an electric arc under helium at a pressure of $1.33 \times 10^4$ Pa. Arc burning affords soot that is condensed on a cold surface. The soot is collected and treated with refluxing toluene or benzene. The extract is concentrated to give a black rasidue containing a mixture of fullerenes $C_{60}$ and $C_{70}$ (~10%–15%). Electron-beam evaporation and laser ablation can be used instead of electric arc sputtering. The diameter of the $C_{60}$ fullerene molecule is 0.72–0.75 nm. Crystallisation of $C_{60}$ affords molecular crystals with a fcc lattice; the unit cell parameter is 1.417 nm. Among carbon nanoparticles fullerene $C_{60}$ is characterised by higher stability, which has been predicted theoretically.[59, 60]

The plasmochemical synthesis was also used for the preparation of other important molecular nanoclusters, such as fullerene-like $C_{48}N_{12}$,[61] the endohedral complex $Ti@C_{28}$ (Ref. 62) and the stable charged cluster $Ti_8C_{12}^+$ with the linear size of ~0.5 nm.[63, 64]

The clusters $M_8C_{12}$, where M = Zr, Hf, V,[65, 66] Cr, Mo or Fe,[67] are called metallocarbohedrenes (Met–Car). In these compounds, transition metal and carbon atoms form a cage-like structure. Metallocarbohedrenes were characterised and the methods for their synthesis were summarised in reviews.[68, 69]

Interestingly, the plasmochemical gas-phase synthesis [63, 65, 66] produced predominantly the clusters $M_8C_{12}$ and $M_mC_n$ (M = Ti, Zr, Hf or V) with a ratio $M:C \approx 1.5-2.0$ rather than nanoparticles of carbides TiC, ZrC, HfC or VC with the structure *B*1. Analogous synthesis in Ta–C and Nb–C systems affords the clusters $Ta_mC_n$ and $Nb_mC_n$, respectively the composition of which is similar to that of $M_8C_{12}$ along with small amounts of nanoparticles $M_mC_n$ ($m \approx n$) with a cubic structure. Conventional plasmochemical synthesis (without laser heating of a plasma) yields only carbide nanoparticles. Thus, the gas-phase synthesis in transition metal–carbon systems can afford both cubic structures and metallocarbohedrene-like structures.

Metallocarbohedrenes are formed at a high hydrocarbon concentration and a high laser power.[70] These conditions favour an increase in the carbon content in the plasma. A decrease in the hydrocarbon concentration or a decrease in the laser power leads to a decrease in the carbon content in the plasma. If carbon is present in a deficient amount, carbide

nanoparticles MC with the cubic structure $B1$ are formed. The carbon content in these particles is lower than that in the molecular clusters $M_mC_n$. This suggests that the formation of cubic or dodecahedral structures in systems M–C under conditions of the gas-phase synthesis is determined primarily by the kinetic rather than thermodynamic factors. The correct answer to the question about the factors responsible for the predominant formation of a particular structure is of practical importance because it allows the targeted synthesis of the desired modification of nanostructured materials.

A version of deposition from a plasma is based on magnetron sputtering, which allows the use of not only metal or alloy cathodes, but also of cathodes made of different compounds, thus decreasing the substrate temperature by 100–200 K. This allows the synthesis of a wider range of nanostructured films. However, the degree of ionisation, the kinetic energy of ions and the deposition rate of the product in the case of magnetron sputtering are lower than those obtained with the use of an arc discharge plasma. Intermetallic $Ni_3Al$ films with an average crystallite size of $\sim$20 nm were synthesised by magnetron sputtering of the $Ni_{0.75}Al_{0.25}$ target and deposition of a metal vapour on an amorphous substrate.[71]

Conventional methods for deposition of films are based on chemical vapour deposition (CVD) and physical vapour deposition (PVD). These methods have long been used for the preparation of films and coatings for different purposes. Generally, crystallites in these materials are rather large in size, but nanostructures can be prepared in multilayer or multiphase CVD films.[8,72] Vapour deposition is generally associated with high-temperature reactions of metal chlorides in an atmosphere of hydrogen and nitrogen or hydrogen and hydrocarbons. The temperature range of deposition of CVD films is 1200–1400 K, and the deposition rate is 0.03–0.2 μm $min^{-1}$. The use of laser radiation leads to a decrease in the deposition temperature to 600–900 K, which is favourable for the formation of nanocrystalline films.

## IV. Deposition from colloidal solutions

Chemical deposition from colloidal solutions is widely used for the preparation of highly dispersed powders as well as of discrete and continuous films. To prepare nanoparticles from colloidal solutions, the chemical reaction between the solution components is interrupted at a particular instant of time,[73] after which the system is converted from the liquid (colloidal) state to the solid (dispersed) state. The method for the preparation of stable colloidal gold solutions and their optical properties were described for the first time by Faraday.[74]

Deposition from aqueous colloidal solutions is used for the synthesis of various metal chalcogenides (sulfides, selenides and tellurides) having semiconducting properties. For example, the synthesis of nanocrystalline sulfide powders involves the reaction of water-soluble metal salts with a sulfidising reagent (a sulfur atom donor). Hydrogen sulfide and sodium sulfide are the simplest sulfidising agents. For example, deposition from a mixture of solutions of cadmium perchlorate and sodium sulfide by the reaction

$$Cd(ClO_4)_2 + Na_2S = CdS\downarrow + 2\,NaClO_4 \qquad (1)$$

affords nanostructured cadmium sulfide. The growth of CdS nanoparticles can be interrupted by a jumpwise increase in pH of the solution.

In the synthesis of sulfide nanoparticles of a specified size, thiocarbamide (thiourea) and its derivatives (for example, thiosemicarbazide, thiocarbazide, thioacetamide, allylthiourea, acetylthiourea and sodium thiosulfate) are used as sulfidising reagents. Each of them is characterised by particular formation rates and properties of the resulting films (precipitates). In addition, each sulfidising reagent is characterised by particular optimal deposition conditions of metal sulfide. Metal sulfides are deposited as a result of the irreversible reaction; the positive chemical affinity serves as the criterion of the spontaneous formation of sulfide.[75] [The chemical affinity is equal to the product of the gas constant and the absolute temperature ($RT$) and the natural logarithm of the ratio of the equilibrium constant of the process under consideration to the product of the concentrations and activities of all components.]

The sizes of PbS particles can be controlled using thiourea and varying the chemical affinity for deposition of the sulfide (Fig. 2). The sulfide particle size, which is equal to the size of coherent X-ray scattering regions at a wavelength $\lambda$, was determined[76–78] by the Williamson–Hall method (Fig. 3) from the dependence of the reduced broadening

$$\beta^*(2\theta) = \frac{\beta(2\theta)\cos\theta}{\lambda}$$

on the scattering vector

$$s = \frac{2\sin\theta}{\lambda};$$

for the quantitative analysis, the X-ray diffraction line profile was described by the pseudo-Voigt function.[77,79]

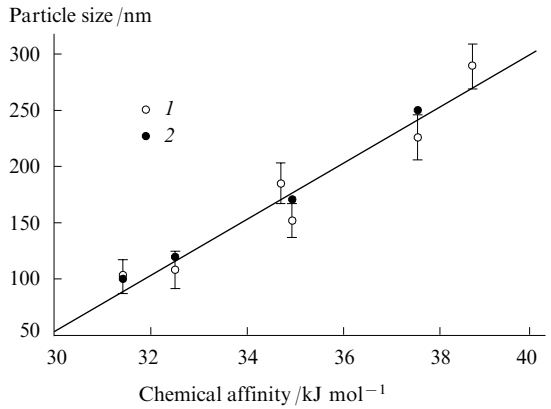



**Figure 2.** Linear approximation (solid line) of the dependence of the particle size (coherent scattering region) on the chemical affinity for deposition of lead sulfide powders.[75]
(*1*) X-Ray diffraction, (*2*) scanning electron microscopy.

The size of cadmium sulfide nanoparticles synthesised by chemical deposition from colloidal solutions with thiourea varied from 2 to 10 nm.[77,80–83] The structures of nanofilms were studied by a new X-ray diffraction method, the so-called X-ray grazing incidence diffraction, which is also called X-ray scattering under total external reflection conditions. This method was used for studying deposition on a substrate and the atomic structures of films several nanometres thick (Fig. 4)[21,78,82] and for confirming the hydroxide mechanism of the formation of cadmium sulfide films.[82]

After deposition of a cadmium sulfide film, the precipitates contained hexagonal prismatic particles several micrometres in size (Figs 5 and 6)[80] where self-organisation of nanoparticles differed substantially from that observed in analogous compounds prepared by chemical deposition[84–87] and from that found in $SiO_2$ (Ref. 88) and $TiO_2$ (Ref. 89). This is because CdS nanoparticles of several nanometres in size, which form a colloidal crystal several micrometres in size, are arbitrarily

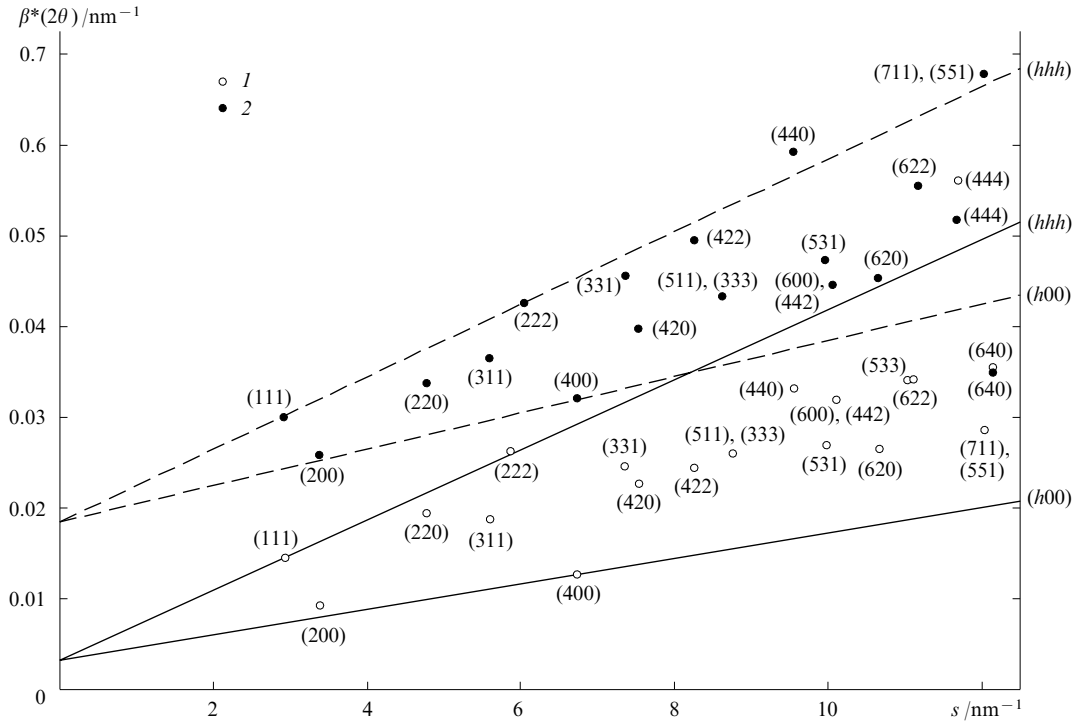



**Figure 3.** Dependence of broadening of reflections $\beta^*(2\theta)$ on the scattering vector ($s$) for submicrocrystalline PbS with a particle size of $300 \pm 50$ nm (*1*) and nanocrystalline PbS with a particle size of $60 \pm 25$ nm (*2*).[75]
The Miller indices for the structure *B*1 are given.

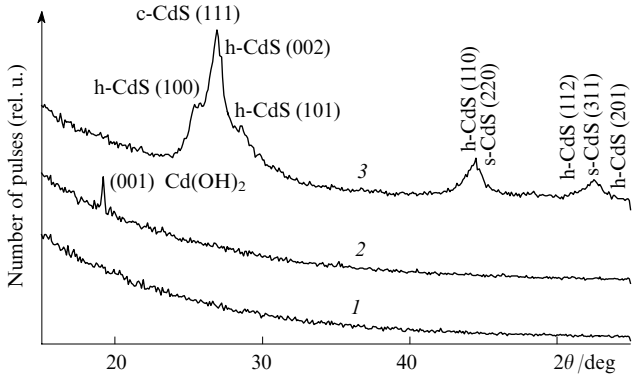



**Figure 4.** X-Ray diffraction spectra of cadmium sulfide films prepared at 325 K by deposition from the reaction mixture during different periods of time.[82]
The concentrations of the components of the reaction mixture /mol litre$^{-1}$: $[CdCl_2]$ is 0.005, $[(NH_2)_2CS]$ is 0.025, $[NH_3]$ is 1.50, [NaOH] is 0.074; the deposition time /min: (*1*) 2, (*2*) 3, (*3*) 3.

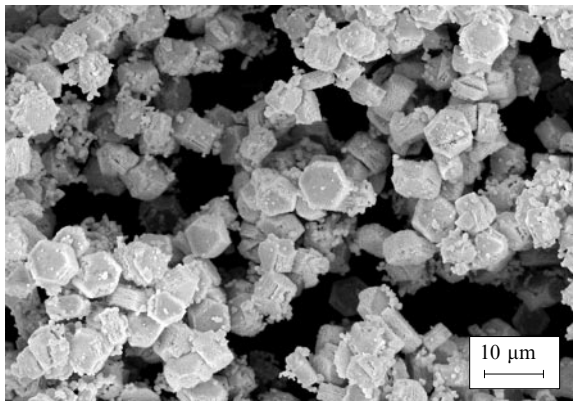



**Figure 5.** A photomicrograph of a precipitate of cadmium sulfide CdS.[80]
Most of particles are well-faceted hexagonal prisms with approximately the same size of $\sim 2.5$ μm.

oriented with respect to each other, are irregular in shape and are different in size. Cadmium sulfide nanoparticles are packed closely together in coagulates with the size of $\sim 150$ nm (Fig. 7).[80]

Self-organisation is a common natural phenomenon.[90, 91] In recent years, the self-organisation processes in chemistry [17, 18] have attracted considerable attention because these processes are intended for the use in nanotechnologies for self-assembly of highly efficient schemes for nanoelectronics. The self-assembly mechanism of nanoparticles remains unclear. Emphasis is given to the elucidation of the nature of forces of interparticle interactions, which result in self-organisation and ordering of nanoparticles to form one-, two- and three-dimensional assemblies.[87] Van der Waals, capillary, electrostatic, steric, *etc*. forces are considered as such forces.

Colloidal metal oxide particles are formed by hydrolysis of salts.[92–95] For example,

$$TiCl_4 + 2\,H_2O = TiO_2\downarrow + 4\,HCl. \qquad (2)$$

Nanocrystalline titanium, zirconium, aluminium and yttrium oxides can be prepared by hydrolysis of the corresponding chlorides or hypochlorites. Titanium oxide nanoparticles can also be prepared by hydrolysis of titanyl sulfate followed by calcination of the amorphous precipitate at 1000–1300 K. Coagulation of nanoparticles can be prevented by addition of polyphosphates, amines and hydroxide ions to colloidal solutions.

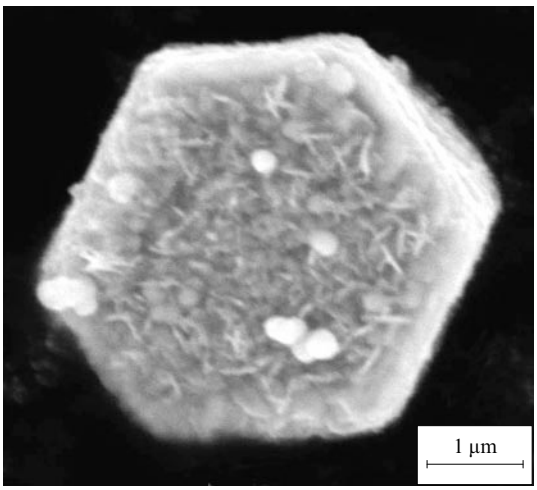



**Figure 6.** A photomicrograph of a typical colloidal crystal prepared by chemical deposition of CdS.[80]
The crystal side length is ~2.5 μm.

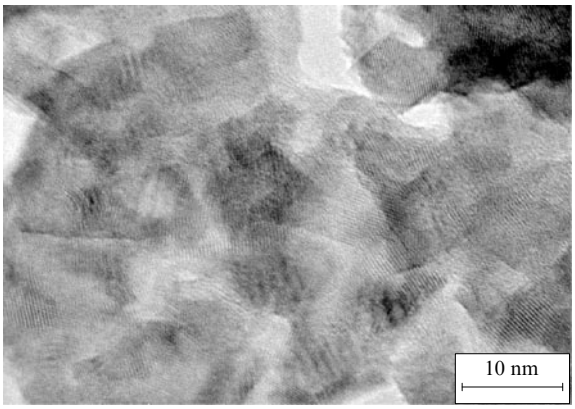



**Figure 7.** A photomicrograph of coagulates in a chemically deposited CdS powder.[80]
Nanoparticles with the size of 7 nm densely fill the volume inside the coagulates.

Deposition from colloidal solutions is highly efficient for the synthesis of isolated nanoparticles and allows the preparation of nanoparticles characterised by a very narrow size distribution.

Metal and semiconductor clusters with a narrow size distribution can be prepared inside pores of molecular sieves (zeolites), isolation of clusters inside the pores being retained upon heating to very high temperatures. This method was used for the synthesis of, for example, the semiconductor clusters $(CdS)_4$.[96] The properties of clusters prepared in zeolite pores were considered in a review.[97] Larger semiconductor nanoparticles can be synthesised upon attachment of additional molecules to the starting clusters pre-stabilised by organic ligands. This synthesis of large nanoparticles can be considered as polymerisation of inorganic compounds.

Isolated nanoparticles can also be obtained by ultrasonic treatment of colloidal solutions containing large particles.

Deposition from colloidal solutions can be used for the synthesis of nanocrystalline heterostructures, *viz.*, nanoparticles with mixed composition where the core and the shell are formed by semiconductors with different structures of the electron levels (for example, CdSe/ZnS or ZnS/CdSe, HgS/CdS, ZnS/ZnO and $TiO_2/SnO_2$). For this purpose, controlled deposition of a semiconductor onto pre-synthesised nanoparticles of a semiconductor of another type should be performed.[98–101]

An important problem encountered in the deposition from colloidal solutions is prevention of coalescence of the resulting particles and clusters. The chemical synthesis of large stabilised metal clusters with the use of colloidal solutions was described in detail in a review.[102] Generally, colloidal particles and clusters are stabilised by ligands L represented usually by polymers. The reaction scheme for the synthesis of ligand-stabilised metal clusters $M_n$ is as follows:

$$n\,M^+ + n\,e^- \longrightarrow M_n \xrightarrow{m\,L} M_nL_m\,. \qquad (3)$$

Metallic gold, platinum and palladium clusters synthesised by this method contain from 300 to 2000 atoms and have cubic or hexagonal close-packed structures. Ligand-stabilised clusters contain the metal core and the external shell formed by the metal atoms that are partially coordinated by ligand molecules. For example, reduction of palladium acetate in acetic acid with hydrogen in the presence of phenanthroline affords stabilised palladium nanoclusters.[103] The phenanthroline molecules form a shell around the core consisting of the palladium atoms (Fig. 8).

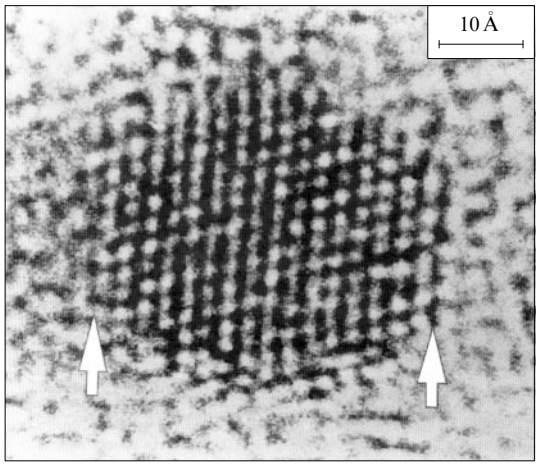



**Figure 8.** A photomicrograph of a stabilised palladium nanocluster formed by seventeen closely packed atom rows and coated by an eight-layer shell composed of phenanthroline molecules.[103]
The cluster boundaries are indicated by arrows.

Highly dispersed powders can be prepared by calcination of precipitates from colloidal solutions consisting of agglomerated nanoparticles at 1200–1500 K. For example, a nanocrystalline silicon carbide powder ($D \sim 40$ nm) was obtained upon hydrolysis of organosilicon compounds followed by calcination in argon at 1800 K.[104] Highly dispersed titanium and zirconium oxide powders are often synthesised by deposition with oxalates.

Nanopowders can also be prepared by cryogenic drying of colloidal solutions.[9, 11] In this case, a solution is sprayed into a chamber containing a cryogenic medium where the solution is frozen as small particles. Then the gas pressure is reduced to a value lower than the equilibrium pressure above the frozen solvent. Then the material is heated (with continuous evacuation of gases) to remove the solvent. As a result, thinnest porous granules possessing the same composition are formed. Calcination of the latter affords powders.

Various nanostructured mixtures can be synthesised by deposition. An efficient procedure was developed [105, 106] for the

synthesis of nanocrystalline composites of tungsten carbide and cobalt, which are intended for the preparation of nanostructured solid alloys. Since the synthesis begins in solution, mixing of the components (WC and Co) occurs at the molecular level. Colloidal solutions of tungsten and cobalt salts [for example, $(NH_4)_6(H_2W_{12}O_{40})\cdot 4\,H_2O$, $CoCl_2$, $Co(NO_3)_2$ and $Co(AcO)_2$] are dried by spraying. Then the resulting powder is subjected to low-temperature carbothermal reduction in a suspended state due to which high dispersity is retained. This technology is covered by a patent [107] under the name the spray conversion process (SCP). A carbidised powder is amorphous. To retard the grain growth and decrease solubility of WC in cobalt, up to 1 mass % of non-stoichiometric vanadium carbide was added to the mixture. The solid alloy prepared from this nanocrystalline composite is characterised by an optimum combination of high hardness and stability. The hardness ($H_V$) of this alloy is as high as 21.5 GPa, whereas the maximum hardness of the alloy with the same composition prepared from a WC powder is at most 19.5 GPa.[105–108] An increase in the percentage of vanadium carbide in the alloy leads to an increase in the hardness and a decrease in the grain size of WC. The size distributions of grains in samples of WC alloys containing 6 mass % Co, which were sintered from a nanostructured mixture with 0.83 mass % VC, and in samples of a WC alloy with 6 wt% Co and an additive of 0.32 mass % VC are shown in Fig. 9.[109] As can be seen from Fig. 9, the average grain size of WC in the alloy prepared from an amorphous nanopowder is 250 nm; in the usual alloy, the grain size is almost twice as large (450 nm).

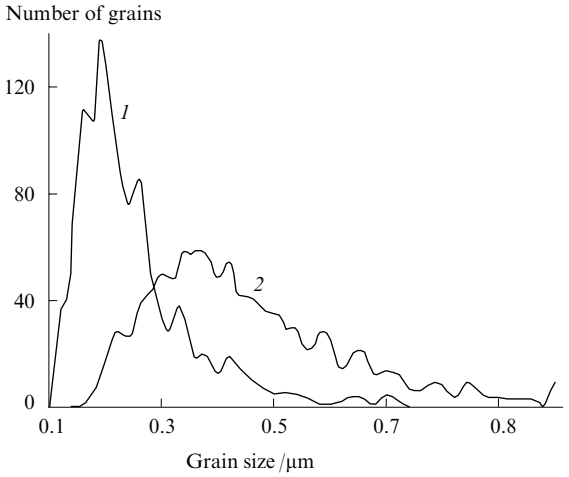



**Figure 9.** The size distribution of grains in samples of a tungsten carbide alloy; 6 mass % Co.[109]
(*1*) An alloy sintered from a nanostructured mixture of WC and Co with 0.83 mass % VC, which was prepared by co-deposition from a colloidal solution followed by drying and carbothermal reduction (the sample contained 1000 grains); (*2*) a usual fine-grain WC alloy with 6 mass % Co and 0.32 mass % VC, the sample contained 948 grains.

Each WC–Co nanoparticle with the size of ~75 μm was demonstrated [109, 110] to consist of several millions of nanocrystalline WC grains with the size < 50 nm distributed in a cobalt matrix (Fig. 10). This nanocrystalline WC–Co powder with a carbide grain size of 20–40 nm is produced in the USA on a commercial scale under the trademark NANOCARB™.

Sintering of a nanostructured mixture of tungsten carbide with 6.8 mass % Co and 1 mass % VC afforded alloys in which 60% of WC grains had sizes of < 250 nm and 20% of WC grains, sizes of < 170 nm. An alloy containing, in addition to tungsten carbide, 9.4 mass % Co, 0.8 mass % $Cr_3C_2$ and

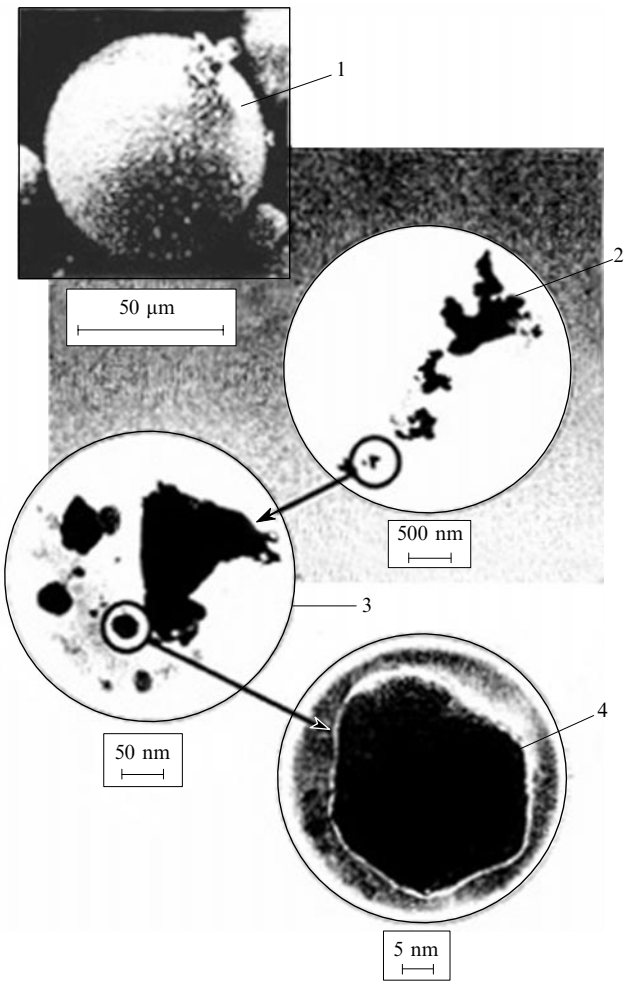



**Figure 10.** Distribution of nanometre-sized tungsten carbide grains in large particles of an amorphous mixture of WC with 6 mass % Co and 0.83 mass % VC, which was prepared by deposition from a colloidal solution followed by drying and carbothermal reduction.[109, 110]
(*1*) A particle of a WC–Co composite powder with the size of 75 μm, (*2*) fragments of the particle after powder milling, (*3*) a polycrystalline cluster composed of WC grains in a cobalt matrix, (*4*) a grain of carbide WC with the size of 30 nm.

0.4 mass % VC had an even finer grain structure. After sintering at 1670 K, 60% of tungsten carbide grains in the alloy had sizes of < 140 nm and 20% of grains, sizes of < 80 nm. Thus, the use of nanostructured WC–Co mixtures synthesised by chemical deposition from colloidal solutions proved to be very efficient for the preparation of nanostructured solid alloys.

Oxide semiconductor films are formed upon deposition onto a support from colloidal solutions. The method involves the preparation of the solution, deposition, drying and annealing. Deposition of oxide nanoparticles afforded ZnO, $SnO_2$, $TiO_2$ and $WO_3$ semiconductor films.[111–115] Nanostructured films containing different semiconductor nanoparticles can be synthesised by co-deposition of the latter. The procedure for the preparation of nanocrystalline $ZrO_2$ films was documented.[116]

Pulsed electrodeposition is an efficient procedure for the application of coatings and films. This method is also widely used for the preparation of nanostructured metals. A support is soaked in a solution containing ions of an element to be precipitated, and the time-variable (pulsed) potential difference is created between the support and the electrode placed in the solution. The pulsed voltage favours the formation of a

homogeneous coating. A study of the influence of the deposition parameters on the structure and properties of a nickel coating [117] demonstrated that the size distribution of grains is narrow, the nickel grain size varying from 13 to 93 nm. Heating of the resulting coating to 380 K did not result in grain growth. The cited study showed also that the grain size and the chemical composition of the nanocrystalline alloy $Ni_{1-x}Cu_x$ deposited at room temperature can be controlled by varying the parameters of the pulsed mode and adding organic compounds to the reaction solution.

## V. Pyrolysis

In the preparation of nanocrystalline metal powders and their compounds by pyrolysis (thermal decomposition), complex organoelement and organometallic compounds, polymers and metal hydroxides, carbonyls, formates, nitrates, oxalates, amides, imides and azides are generally used as the starting compounds. These compounds contain all or almost all chemical elements, which should be present in the target product. Heating of the starting compounds to a particular temperature results in their decomposition to form the target product and evolution of gaseous compounds.

Highly dispersed metal powders are synthesised by thermal decomposition of various salts.[118] For example, metal powders with an average particle size of 100–300 nm were prepared by pyrolysis of iron, cobalt, nickel and copper formates under vacuum or in an inert gas at 470–530 K. Other combinations of pyrolysis and condensation are also used for this purpose. Decomposition of organometallic compounds occurs in a percussion fuse, after which free metal atoms are condensed from a supersaturated vapour, or during supersonic gas flow from a chamber through a nozzle into vacuum.[119] The preparation of nanocrystalline metal powders by reduction of metal hydroxides, chlorides, nitrates and carbonates in a hydrogen flow at < 500 K can be considered as a modification of pyrolysis. Low impurity content and a narrow size distribution of particles are advantages of this method.

Thermal decomposition combined with reduction is used for the preparation of supported metal catalysts. This technology is widely employed in industry. In this case, a porous material (silica gel, zeolite, *etc.*) is impregnated with a solution of hydroxide or another compound of the required metal. The impregnated porous support is dried and then calcined in a hydrogen flow to reduce the metal. As a result, catalytically active metal nanoparticles are formed in pores of the support.

However, pyrolysis is most often used for the preparation of nanocrystalline powders of ceramic materials, such as various oxides, carbides, nitrides, borides, carbonitrides, borocarbides, borocarbonitrides, *etc.*

The synthesis of oxide nanomaterials starting from metal carboxylates and their chemical modification products by ethylene glycol was documented.[120] The compound $Ti(OCH_2CH_2O)_2$ proved to be an efficient precursor for the synthesis of titanium dioxide nanofibres with a diameter from 20 to 100 nm.[121] Titanium glycolate nanofibres were synthesised by heating hydrated titanium dioxide $Ti(OH)_4$ with ethylene glycol in air. Then titanium glycolate nanofibres were subjected to thermal decomposition in air at a temperature from 400 to 900 °C to prepare $TiO_2$ nanofibres. Depending on the thermal decomposition temperature, titanium dioxide had a crystal structure of either anatase or rutile, the morphology of the precursor being retained.

A nanocrystalline powder of titanium carbide TiC can be synthesised by pyrolysis of the coordination organometallic compound $(\eta\text{-}C_5H_5)_2TiMe_2$ under argon or by pyrolysis of the polymer $[(C_6H_4O_2)_2Ti]_n$ under argon with the use of hydrogen as the reducing agent.[122]

Nanocrystalline SiC powders can be prepared by thermal decomposition of polycarbosilanes and polycarbosiloxanes; nanocrystalline silicon nitride $Si_3N_4$ is produced by pyrolysis of polysilazanes.[123–125] Since polycarbosiloxanes contain oxygen atoms, their pyrolysis is performed under hydrogen according to the scheme

$$\text{—[SiMe}_2\text{O]—}_n \xrightarrow{H_2} \text{SiC}. \quad (4)$$

Initial heating is carried out using a high-temperature plasma or laser radiation followed by additional annealing of pyrolysis products at ~ 1600 K.

Nanocrystalline boron carbide $B_4C$ is obtained upon decomposition of poly(vinylpentaborane) $[C_2H_3(B_5H_8)]_n$. Polyborazine-, polyborazole- and polyvinylborazine-type boron-containing polymers were suggested [125] for the use in the synthesis of highly dispersed boron nitride powders and as additives to a titanium powder for the synthesis of nanocrystalline composites $TiN + TiB_2$. A nanocrystalline aluminium nitride powder with an average particle size of 8 nm was synthesised by decomposition of $[Al(NH_2)_3NH]_n$ in ammonia at 900 K.[126]

To stabilise the composition and structure of the powders prepared by pyrolysis of monomeric and polymeric compounds, it is necessary to perform their additional annealing; the annealing temperature of nitrides and borides varies from 900 to 1300 K and that of oxides and carbides, from 1200 to 1800 K. The main drawback of thermal decomposition is that the selectivity of the reaction is rather low so that the reaction product represents a mixture of the final product and intermediates.

Nowadays, thermal decomposition is applied to the synthesis of multicomponent amorphous and nanocrystalline ceramic materials. For example, the complex ceramic material $Si_3B_1C_{4.3}N_2$ was synthesised by decomposition of polyvinylsilazane $(B[C_2H_4SiMeNH]_3)_n$ at 523 K for 1 h and at 623 K for 3 h followed by milling of the product and its dehydrogenation at 1673 K for 2 h.[127] The influence of annealing on nanocrystallisation and the free volume change in ceramics were examined in detail for the Si—C—B—N system by X-ray diffraction methods and positron annihilation.[128]

A nanostructured mixture of WC and Co can be prepared by pyrolysis of various precursors.[122] In particular, heating can simultaneously afford WC and Co

$$(NH_4)_8[H_2Co_2W_{11}O_{40}] \longrightarrow WC + Co, \quad (5)$$

$$[CoEn]_3WO_4 \longrightarrow WC + Co, \quad (6)$$

where En is ethylenediamine.

## VI. Mechanosynthesis

Mechanosynthesis is one of the most efficient 'dry' chemical technologies requiring no or a minimum amount of solvents for chemical reactions. The mechanical treatment of solid mixtures is accompanied by dispersion of substances, acceleration of the mass transfer, mixing of the components at an atomic level and, as a consequence, activation of their chemical reaction.[129, 130] The mechanisms of mechanochemical reactions are characterised by the involvement of many steps. The most important steps are as follows: initial deformation of the crystal structures of the reactants, the formation, accumulation and interactions of point and linear defects, disintegration of substances, the formation of metastable states in the contact zone of different phases, chemical homogenisation and relaxation of the reaction products to the equilibrium state.[131] The reactivity of solids in the course of their deformation and decomposition is the subject of mechanochemistry.

Mechanical milling can result in a decrease in the size of microcrystalline blocks to 10 nm (and smaller), which is equivalent to a decrease in the diffusion length necessary for the reaction.[129] Simultaneous mechanical treatment of several components of the mixture causes deformation mixing and mechanochemical reactions. The characteristic features of low-temperature mixing of solid reactants associated with the formation of intermediate metastable states and the possibilities of the mechanochemical synthesis of various compounds were covered in detail in the reviews.[129, 130]

The mechanical milling is an efficient procedure for the preparation of large amounts of nanopowders of various materials, such as metals, alloys, intermetallides, ceramics and composites. Complete solid-state solubility of elements mutual solubility of which under equilibrium conditions is negligibly small can be achieved by mechanical milling and mechanical fusion.[132, 133] Various mills (reactors) in which the specific mechanical energy imparted to a powder can be as high as $10^2 - 10^3$ kJ $g^{-1}$ are most popular for mechanical activation of powders and mechanochemical processes.

During mechanical milling of powders, the plastic deformation is developed by the dislocation mechanism and it is initially localised in slip bands containing multiple dislocations. As a particular stress level is achieved, these dislocations annihilate, are combined and recombine as small-angle grain boundaries, which separate individual grains, entrapping impurity atoms. In this step of milling, particles with a diameter of 20 – 30 nm are formed, and their number increases as the particles are ground. In plastic metals, intergrain boundaries are formed by the polygonisation mechanism.[134] In the next step of milling, the orientation of individual crystallites with respect to each other becomes random due to a slip along the grain boundaries. This behaviour in the course of milling is typical of metals and intermetallides with a bcc lattice.[133]

The mechanical action during milling of materials is pulsed in character. Hence, the stress field does not act during the entire residence time of particles in the reactor but only at the instant of their collision. During a short period after the collision, partial relaxation occurs. Hence, the character of formation of the stress field in time and the kinetics of subsequent relaxation processes should be taken into account in the mechanochemical synthesis. The mechanical action is not only pulsed, but also local, because it occurs not in the total bulk of the solid, but only where the stress field appears and then relaxes.

Let us consider some results of milling and mechanochemical synthesis with the use of high-energy planetary and vibration mills. A nanocrystalline powder of barium titanate ($BaTiO_3$) with an average particle size of 25 nm was prepared by the mechanical treatment in a planetary ball mill.[135] According to the results of electron microscopy, $BaTiO_3$ nanoparticles contain almost no dislocations. Nanoparticles were combined to form dense aggregates up to 1 μm in size, which in turn form large agglomerates $> 2$ μm in size. The agglomeration is a characteristic property of nanocrystalline powders prepared by mechanical milling.

Mechanochemical synthesis of transition metal boride, carbide, silicide and sulfide powders from powdered mixtures of metals with boron, carbon, silicon and sulfur, respectively, was performed by the so-called explosion method in vibration mills.[136] In essence, the explosion mechanosynthesis is analogous to the self-propagating high-temperature synthesis; however, unlike the latter method, the fast reaction in the explosion mechanosynthesis is initiated by mechanical activation of powders of the starting components (metal and carbon, boron, silicon or sulfur) for a few minutes rather than by a short-term powerful thermal pulse. X-Ray diffraction and electron microscopic studies of boron, titanium, zirconium, hafnium, vanadium, tantalum and tungsten carbide powders prepared by the mechanochemical synthesis in eccentric and planetary ball mills demonstrated that the average particle size in these powders varied from 6 to 20 nm.[137] Metal powders were mechanically milled in planetary and vibration mills under oxygen and nitrogen, respectively to prepare nanocrystalline oxides and nitrides with a particle size of several nanometres.[138]

The mechanochemical synthesis of nanocrystalline carbides TiC, ZrC, VC and NbC with an average particle size of $7 \pm 1$ nm was carried out by 48-h milling in a planetary ball mill of a mixture of metal and carbon powders.[139] The formation of carbides starts 4 – 12 h after the beginning of milling. The study of thermal stability of dispersed nanocrystalline carbides demonstrated [139] that niobium carbide is the most heat-resistant of all the synthesised carbide nanopowders. The grain size of NbC increases from 7 – 10 to 30 nm as the temperature increases from 300 to 1300 K. Vanadium carbide is the least thermally stable. Extensive recrystallisation at 1000 – 1200 K resulted in the VC grain growth to 90 nm.

Vibration ball milling of mixtures of metal powders for 300 h afforded nanocrystalline (the grain size was 5 – 15 nm) Fe – Ni and Fe – Al alloys with bcc lattices.[140]

The synthesis of amorphous nanocrystalline $Ni_3Al$ powders by mechanical milling of an ordered intermetallic alloy $Ni_3Al$ was documented.[141] The coarse-grained (with a particle size of $\leqslant 45$ μm) powder had an ordered $Cu_3Au$-type cubic structure ($L1_2$) with a long-range parameter of 0.96. After its ball milling for 5 h, superstructure reflections in the X-ray diffraction pattern disappeared (complete ordering of the powder) and the structure reflections corresponding to the fcc lattice broadened. The average crystallite size and the lattice strains were estimated [141] from the broadening of the structure reflections of a $Ni_3Al$ powder by the Willamson – Hall method.[142 – 144] After 5-h milling, the average crystallite size was 19 nm, and the microstrain was $2 \times 10^{-4}$ (0.02%). An increase in the milling time to 50 h led to a further broadening of the most intense structure reflections (111) and (200) and the disappearance of other structure reflections. The size of the coherent scattering regions decreased to 8 – 10 nm. A study of the milled powder by scanning and transmission electron microscopy demonstrated that the nanoparticle size was 2 – 3 nm, and the electron diffraction pattern for nanoparticles is typical of an amorphous state. Thus, mechanical milling of a coarse-grained powder of the ordered intermetallide $Ni_3Al$ initially resulted in its disorder (the formation of a disordered fcc alloy with an $A1$-type structure) followed by the formation of a nanocrystalline fcc alloy and, in the final step of milling, an amorphous $Ni_3Al$ powder with an average nanoparticle size of $\sim 2$ nm.

The mechanochemical synthesis can be combined with the synthesis of a nanostructured mixture.[145] In an argon-filled ball mill, a nanostructured mixture of cobalt and tungsten carbide grains with an average size of 11 – 12 nm is formed after milling of a mixture of course-grained ($\sim 75$ μm) tungsten, graphite and cobalt powders for 100 h. In the solid alloy prepared by cold pressing followed by sintering of this mixture at 1310 K, most of WC grains had a size of $< 200$ nm, *i.e.*, they were several times smaller than those in usual alloys of the same composition. The sintered samples of the alloy had a hardness of $\sim 18$ GPa and a relative density of 80% of the theoretical value. It was hypothesised [145] that the lower sintering temperature of a nanostructured powdered WC – Co mixture compared to that of a coarse-grained mixture is a consequence of the lower melting point of nanocrystalline cobalt compared to that of the coarse-grained metal.

A complex methodologically correct study of the mechanosynthesis of a nanocrystalline cubic titanium carbide powder was documented.[146] The results of this study deserve a more

detailed discussion. Metallic titanium and graphite powders in a ratio of 44 : 56 were milled in a sapphire ball mill at room temperature under argon.

After milling for $2 \times 10^3$ s, the X-ray diffraction pattern of the reaction mixture (Fig. 11) showed only broad reflections corresponding to elemental Ti and C. After milling for $11 \times 10^3$ s, the reflections corresponding to graphite almost disappeared; after milling for $15 \times 10^3$ s, reflections of a new cubic phase with the structure $B1$ (titanium carbide) appeared. This is consistent with the results of investigation [139] in which the formation of carbide phases was observed after milling of powdered mixtures of transition metal and carbon for four–six hours. An increase in the milling time to $4 \times 10^4$ s led to the complete disappearance of X-ray reflections of titanium metal and an increase in the intensities of reflections of titanium carbide. Further increase in the milling time was accompanied by an increase in mechanical deformation of powder particles and a sharp decrease in the grain size, as evidenced by a noticeable broadening of X-ray reflections. Milling for $72 \times 10^4$ s afforded nanocrystalline titanium carbide and subsequent increase in the milling time to $10^6$ s did not lead to changes in the resulting carbide.

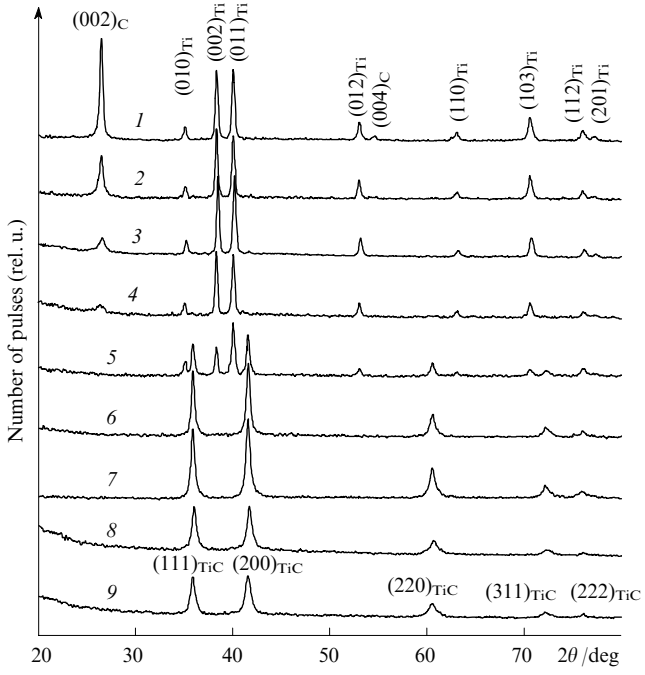



**Figure 11.** Changes in the X-ray diffraction pattern of powdered 44 Ti + 56 C mixtures prepared at different milling times.[146]
The changes in the X-ray diffraction patterns are associated with changes in the phase composition resulting from the formation of titanium carbide and with disintegration of carbide particles to nanometre sizes. The milling time /s: (*1*) $2 \times 10^3$, (*2*) $6 \times 10^3$, (*3*) $8 \times 10^3$, (*4*) $11 \times 10^3$, (*5*) $15 \times 10^3$, (*6*) $22 \times 10^3$, (*7*) $4 \times 10^4$, (*8*) $8 \times 10^4$, (*9*) $72 \times 10^4$.

The changes in the grain size of powders during milling are illustrated in Fig. 12. The formation of nanocrystalline titanium carbide involves four steps presented in Fig. 13. The starting powder (Fig. 13 *a*) consists of randomly distributed particles of different size and shape. In the first step (the milling time up to $11 \times 10^3$ s), very large (with the size of $\sim 1$ mm) composite Ti/C particles are formed (Fig. 13 *b*). A metallographic study demonstrated that these particles consist of numerous titanium and carbon layers. The second step (the milling time from $11 \times 10^3$ to $2 \times 10^4$ s) involves a solid-phase

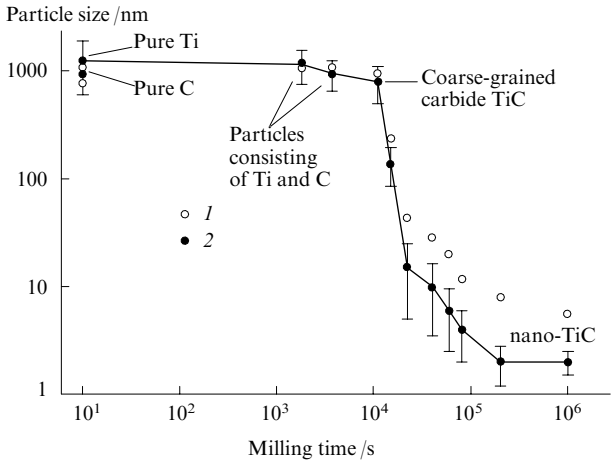



**Figure 12.** The plot of the particle size of a milled powder containing titanium and carbon particles (44 : 56) *vs.* the milling time in the mechanosynthesis of titanium carbide.[146]
(*1*) The particle size determined from the broadening of X-ray reflections; (*2*) the particle size determined by electron microscopy.

reaction during which titanium and carbon react almost completely with each other to form large titanium carbide grains from 800 to 1000 nm in size. In the third step (the milling time from $2 \times 10^4$ to $8 \times 10^4$ s), extensive dispersion of large titanium carbide grains affords a finely dispersed powder with a rather broad size distribution of grains (from 5 to 100 nm); the carbide grains form particles with the size of 5–10 μm (Fig. 13 *c*). In the last step (the milling time from $8 \times 10^4$ to $1 \times 10^6$ s), the nanocrystalline powder is homogenised with respect to the grain size resulting in the average grain size of $\sim 2 \pm 1$ nm; the grains agglomerate to form spherical particles with the size no larger than 300 nm (Fig. 13 *d*).

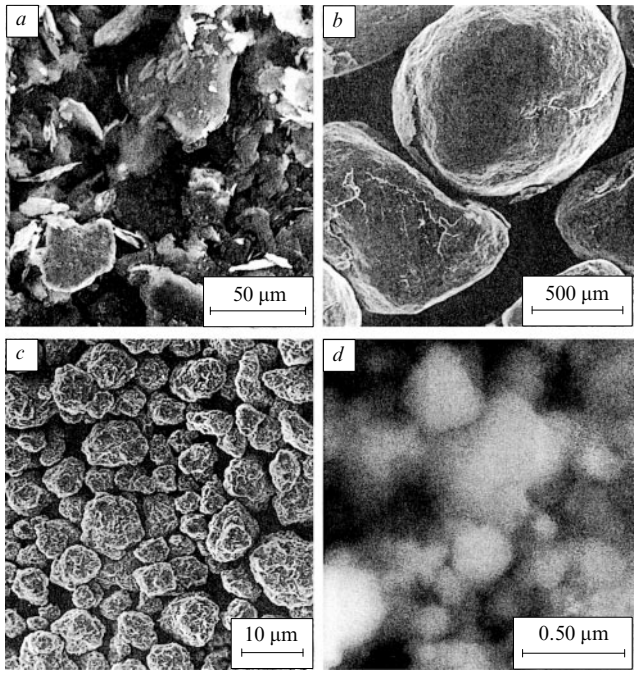



**Figure 13.** Photomicrographs of particles of the staring powdered mixture of titanium and carbon (44 : 56) (*a*) and a powder after ball milling during different periods of time (*b*–*d*) see the text.[146]

The titanium carbide powder thus prepared was sintered in an activated plasma. The sintering afforded compact titanium carbide samples with high densities (up to 5.2 g $cm^{-3}$) and hardnesses (up to 3.2 GPa), the average grain size of $< 70$ nm being retained.

The results of the study [146] demonstrated high efficiency of the mechanosynthesis of nanocrystalline titanium carbide. However, it should be noted that the authors' hypothesis that the composition of the starting mixture is identical with that of the synthesised titanium carbide casts doubt, because if this were the case, the superstoichiometric carbide $TiC_{1.27}$ or the carbide $Ti_{0.79}C_{1.00}$ with a defect metal sublattice would be synthesised. The lattice period of the synthesised titanium carbide (0.4326 nm) is somewhat smaller, whereas the measured density (5.2 g $cm^{-3}$) is higher than the corresponding parameters (0.4328 nm and 4.91 g $cm^{-3}$, respectively) of the conventional stoichiometric carbide $TiC_{1.0}$. An excess of carbon atoms in the carbide and its high density can be attributed to the presence of interstitial carbon atoms in the structure $B1$.

## VII. Detonation-induced synthesis

Shock waves is yet another type of mechanical action that creates the conditions for both disintegration of the starting compounds and the synthesis of the final product. Detonation of explosives (the explosion energy) is widely used for performing phase transitions and the synthesis of new compounds. The detonation-induced synthesis of nanopowders proceeds under dynamic conditions where kinetic processes play an important role.

The detonation-induced synthesis of diamond from rhombohedral graphite using a shock wave (the pressure of up to 30 GPa was achieved) was documented.[147] The shock-wave treatment of mixtures of graphite and metals (the duration of a shock wave was 10–20 μs and the produced pressure was 20–40 GPa) afforded [148] diamond powders. These powders were shown to contain single crystals with the size no larger than 50 nm along with assemblies and tightly bound agglomerates with the size of up to 5 μm consisting of individual crystals with sizes of 1–4 and 10–160 nm, respectively.

The 'dry synthesis' based on detonation of condensed carbon-containing explosives with a negative oxygen balance followed by cooling of the detonation products under an inert atmosphere was documented.[149, 150] Presently, this process is used for industrial production of diamond nanopowders for different technical purposes. The synthesis is performed in explosion chambers with a volume of no smaller than 2–3 $m^3$. In the so-called 'aqueous synthesis', which is another version of the detonation-induced synthesis of diamond powders, the diamond particles are cooled with water.

Diamond powders are formed in the zone of chemical decomposition of the starting compounds within $< 0.4$ μs. These powders consist of compact cubic particles with an average size of $\sim 4$ nm. Large (up to 1 μm) diamond particles can be prepared with the use of powerful explosives.[151]

The detonation-induced synthesis of various morphological forms of carbon as well as of aluminium, magnesium, titanium, zirconium and zinc oxide nanopowders was described.[152, 153] A shock wave passing through a layer of the starting compound (highly porous metal, a chemical compound or a metal hydroxide sol or gel) causes compression and heating of highly porous metals or decomposition of the starting compound to form oxide followed by stabilisation of oxide phases. After the escape of the shock wave on the free surface of the starting compound, materials disperse in the gas atmosphere of the explosion chamber. In a $CO_2$ atmosphere, carbon nanotubes, spherical carbon particles and thread-like MgO crystals were obtained. The average diameter of thread-like MgO crystals was 60 nm, and the length to diameter ratio reached 100.

Reactions with chemical compounds as the starting reactants are performed with the use of gaseous and liquid media neutral with respect to the final products, due to which the compounds are rapidly cooled and high-temperature and metastable crystal modifications are stabilised. For example, an yttrium oxide-stabilised cubic $ZrO_2$ nanopowder was synthesised [152, 153] by the detonation method. The average particle size was 30 nm.

## VIII. Self-propagating high-temperature synthesis

Self-propagating high-temperature synthesis (SHS) is rapidly propagating combustion of solids (of a metal and carbon in the synthesis of carbides or of a metal under nitrogen in the synthesis of nitrides) at a temperature from 2500 to 3000 K.[154, 155] Since the particle size in the self-propagating high-temperature synthesis products is usually 1–5 μm, it was believed that this method is inapplicable to the preparation of compounds in the nanocrystalline state.

It was suggested [156] that titanium carbide nanopowders would be synthesised by the SHS method in the presence of an inert diluent preventing the particle growth, *e.g.*, using a $Ti + C + m\,NaCl$ mixture, where $m = 0.2–0.7$. The particle sizes of the starting Ti, C and NaCl powders were at most 50, 0.1 and 150 μm, respectively. Pellets with a diameter of 30 mm and a height of 40 mm were pressed from the powder mixture. The synthesis was carried out in a standard reactor under argon at a pressure of 0.5 MPa. Combustion was initiated by a current pulse (the voltage was 15–20 V and the pulse duration was 1.0–1.5 s), which was supplied to the sample with a tungsten wire. The combustion temperature decreased from 2500 to 1950 K C as the amount of sodium chloride increased (as $m$ changes from 0.2 to 0.7).

The combustion was accompanied by spontaneous homogenisation of the staring mixture due to melting of Ti and NaCl. A microscopic study demonstrated that the resulting titanium carbide particles are distributed in a NaCl melt and are isolated from each other by a thin layer of this melt, which prevented their further growth. No intermediate phases were found. The titanium carbide particle size decreased with the increase in the amount of NaCl in the starting mixture. After washing off NaCl, the titanium carbide powder was studied by X-ray diffraction and electron microscopy. The resulting titanium carbide had the cubic structure $B1$ with a lattice parameter of 0.433 nm. The powder consisted of particles of irregular shape with a size from 20 to 300 nm; the average particle size was $\sim 100$ nm. The optimum amount of NaCl for the synthesis of titanium carbide nanoparticles ($m$) was found [154] to be 0.4 (or $\sim 30$ mass%). The chemical composition of titanium carbide synthesised in the study [156] was not determined.

## IX. Compaction of nanopowders

A method for the preparation of compact dense three-dimensional (3D) nanocrystalline materials named after Gleiter, who was the first to suggest this method,[157] involves the following steps: condensation of nanoparticles under a low-pressure inert gas atmosphere, deposition of particles onto a cold surface of a rotating cylinder and scraping of nanoparticles from the cylinder surface to a collector.[158] After evacuation of the inert gas from the chamber, a nanocrystalline powder was prepressed (under a pressure of $\sim 1$ GPa) and finally pressed under a pressure of up to 10 GPa. This method can be used for the preparation of cylinders with a diameter from 5 to 15 mm, a thickness of 0.2–3.0 mm and a density of 70%–90% of the theoretical density of the corresponding material. In partic-

ular, the density of nanocrystalline metal powders reaches 97%; the density of nanoceramics, 85%.[3] Depending on the evaporation and condensation conditions, compact nanomaterials consist of particles with an average size from 1–2 nm to 80–100 nm. This method was applied to the preparation of compact nanocrystalline nickel with an average particle size of 60 nm.[159]

The contact of substances with the environment in the synthesis of nanopowders and their pressing is excluded due to which compact nanocrystalline samples remain uncontaminated. The apparatus described in the papers cited [157, 158] can be used for the preparation of compact nanocrystalline oxides and nitrides.

The porosity of nanoceramics prepared by pressing of powders is determined primarily by the pores located at triple joints of crystallites and the grain boundaries.[2] Powders of lower dispersity are less compressible.[160] A uniform porosity distribution is achieved by pressing ceramics at high temperature at which no extensive recrystallisation occurs. For example, conventional sintering of a highly dispersed zirconium oxide powder with a particle size of 40–60 nm at 1370 K for 10 s afforded a material with a relative density of 72% and an average grain size of 120 nm. Hot pressing at the same temperature under a pressure of 1.6 GPa afforded a material with a relative density of 87% and an average grain size of 130 nm.[161] Compact oxide $ZrO_2$ with a relative density of >99% and an average grain size of 85 nm was obtained when the temperature was lowered to 1320 K and the sintering time was increased to 5 h.[162] The most dense (with a relative density of 98%) samples of titanium nitride could be obtained by sintering samples pressed from finely dispersed nanopowders with a grain size of ~ 8–25 nm and a minimum deviation of the grain size from these values.[163]

Sintering of powders at a high (up to 10 GPa and higher) pressure holds promise for the preparation of dense compact finely grained materials.[164, 165] For example, a TiN powder with an average particle size of 40 nm was sintered at 3 and 4 GPa at a temperature from 1000 to 1800 K. The maximum density of sintered samples was achieved at 1670 K. An increase in the pressure was accompanied by an increase in the density to 94% of the theoretical value, the crystallite size was 200–300 nm. It should be noted that the crystallite size in samples sintered at 1400–1500 K was at most 60 nm, and the relative density of samples was as high as 92%–93%.

Pressing followed by high-temperature sintering holds promise for the synthesis of compact nanomaterials, particularly, of ceramic materials. To prevent grain enlargement during sintering of pressed samples, it is necessary to use high-density pressing and low sintering temperature $T \leqslant 0.3T_m$ ($T_m$ is the melting point). The preparation of high-density compact materials presents a serious problem because it is difficult to press nanopowders by conventional static pressing methods. Poor compressibility of nanopowders is associated with adhesion forces the contribution of which to interparticle interactions sharply increases with a decrease in the particle size.

The magnetic pulse method is rather efficient for compaction of nanopowders.[166–168] This method consists of concentrating the force action of magnetic field of powerful pulse currents, resulting in the appearance of compression waves with an amplitude of up to 5 GPa and a duration of a few microseconds. The parameters of compression waves can rather easily be controlled in this method. The magnetic pulse pressing is environmentally safe, it is much safer than dynamic methods.

Unlike stationary pressing methods, the magnetic pulse method results in extensive heating of powders due to rapid energy release caused by particle friction during packing under the action of a compression wave. If particles are sufficiently small ($\leqslant$300 nm), the time of their heating is substantially shorter than the characteristic duration of pulse compression waves. Under the same pressure, the magnetic pulse method sometimes allows the preparation of denser compact samples than those prepared by stationary pressing. Aluminium nitride powders prepared by electric explosion (see below) are pressed by the magnetic pulse method under a pressure of 2 GPa to the density of 95% of the theoretical value; $Al_2O_3$ powders, to the relative density of 86%. This method is applied to the preparation of articles of different shape, which, as a rule, require no additional mechanical treatment. In particular, articles of a complex shape with a density of >95% of the theoretical value were formed from powders of superconducting oxide ceramics.[167] In the general case, interparticle forces are efficiently overcome in the case of rapid motion of a powder medium under the action of pressure pulses due to which the resulting samples have higher density than samples prepared by static pressing. Heating of nanopowders lasts for a short while, which favours a decrease in its recrystallisation at high temperature and the retention of a small particle size.

The magnetic pulse method was used for pressing nanocrystalline $Al_2O_3$ (see Refs 169 and 170) and TiN powders.[171] An increase in the pressing temperature to ~900 K was demonstrated [171] to be more efficient than an increase in the pressure in cold pressing. Compact samples of nanocrystalline titanium nitride with a grain size of ~80 nm and a density of ~83% of the theoretical value were prepared under a pulsed pressure of 4.1 GPa at 870 K. A decrease in the pressing temperature to 720 K was accompanied by a decrease in the density to 81%.

A comparative study of compaction of ultradispersed TiN powders by magnetic pulse pressing, high-pressure pressing and conventional pressing was reported.[172] The average particle sizes of the starting powders were 70 and 80 nm. A decrease in the particle size led to a decrease in the degree of compression of samples. An increase in the pressing pressure was accompanied by an increase in the relative density. An increase in the density becomes slower at a pressure of >4 GPa, the density being no higher than 85% even at 7 GPa. It was noted that cold pressing according to different procedures gives very similar results at a pressure of >1 GPa. At 1 GPa, the density of samples prepared by the magnetic pulse method appeared to be somewhat lower than that of samples prepared by static pressing.

Gas-tight ceramic tubes with an external diameter of up to 15 mm and a length of up to 100 mm were produced from nanopowders by radial magnetic pulse pressing.[173] Powders were placed in a cylindrical gap between a rigid metallic rod and an external cylindrical copper shell. The pressing was performed by radial compression of the external shell under current pulses, the developed pulse pressure being 2 GPa. Aluminium oxide nanopowders and an $Y_2O_3-ZrO_2$ mixture with an average particle size of 10–30 nm were used as the starting materials. Radial magnetic pulse pressing of these nanopowders afforded tubes with a relative density of ceramics of >95%.

Ceramic nanopowders can be compacted by dry cold ultrasonic pressing.[174, 175] Under the action of an ultrasonic field with a power of several kilowatts, interparticle frictions and frictions between particles and walls of the press form decrease, agglomerates and large particles are disintegrated, the surface activity of the powder particles increases and the volume distribution of particles becomes more uniform. This results in an increase in the density of pressed articles, acceleration of diffusion processes, limitation of the grain growth in subsequent sintering and retention of the nanostructure. For example, ultrasonic pressing of an $Y_2O_3$-stabilised $ZrO_2$ nanopowder followed by sintering of samples in air at 1923 K afforded a ceramic material with a relative density of ~90%.

The average particle size in the initial nanopowder was $\sim 50$ nm.

An interesting procedure for sintering of ceramic compact nanomaterials based on heating of sintered samples with the use of microwave radiation was documented.[176, 177] Heating is performed by millimetre-range radiation with frequencies from 24 to 84 GHz in a technological gyrotronic device with a power of several kilowatts. The volume energy absorption of microwave radiation provides simultaneous uniform heating of samples because the heating rate is not limited by heat conductivity, as opposed to conventional sintering methods. This allows the preparation of sintered ceramics with a homogeneous microstructure.

Compact samples of $Al_2O_3$ were prepared by cold isostatic and magnetic-pulse pressing of a nanopowder with an average particle size of 26 nm.[177] The relative densities of the pressed samples were 52% and 70%, respectively. Microwave sintering at maximum temperatures of 1570 and 1770 K afforded samples of $Al_2O_3$ with a density of 99% of the theoretical value and an average crystallite size of $\sim 80$ nm.

Conventional sintering methods do not always allow strong connection of different ceramic materials. For example, it is impossible to prepare a mechanically stable composite of $ZrO_2$ and $Al_2O_3$, which is reqired for the design of devices such as thermal barriers, by conventional methods. This problem can be solved with the use of nanocrystalline materials and microwave sintering.[177] Oxides $ZrO_2$ and $Al_2O_3$ are bound to each other with the use of a sintered interlayer made from the nanosized composite ceramic material 60 vol.% $ZrO_2$ + 40 vol.% $Al_2O_3$ with an average grain size of 100 nm. The relative density of the interlayer was 96% – 98% of the theoretical value. Microwave heating of the $ZrO_2$/interlayer/$Al_2O_3$ structure over a short period of time to 1700 K afforded a stable composite consisting of oxides $ZrO_2$ and $Al_2O_3$.

## X. Crystallisation of amorphous alloys

The above-described methods are based on the assembly principle, *i.e.*, belong to 'bottom-up' nanotechnologies. Methods of 'top-down' technologies are described below.

Nanostructures can be formed in amorphous alloys by crystallisation.[178] Amorphous metal alloys can be prepared by rapid (at a rate of $\geqslant 10^6$ K $s^{-1}$) cooling of alloys on the surface of a rotating disc or drum. This method is called spinning. Nanostructures are created by annealing in such a way as to form a large number of crystallisation centres and the crystal growth rate is low.

The amorphous magnetically hard alloy $Fe_{90}Zr_7B_3$ can be referred to as an example.[178] The amorphous alloy was prepared by spinning and then subjected to relaxation annealing at 673 K for 2 h. A nanocrystalline structure formed when the alloy was additionally annealed at 873 K under vacuum ($10^{-5}$ Pa) for 1 h. The transformation of the $Fe_{90}Zr_7B_3$ alloy from the amorphous to the nanocrystalline state results in a change in the X-ray diffraction pattern (Fig. 14): very broad diffuse X-ray reflections become sharp and narrow.[178] The grain size of the crystalline bcc phase α-Fe(Zr) that is formed in the amorphous matrix was $\sim 10$ nm (results of high-resolution electron microscopy). Considerable attention was given to investigation of the structure of an amorphous matrix containing α-iron nanoparticles.[178] In particular, a study of the atomic structure of the matrix by modern electron – positron annihilation methods revealed a high content of zirconium concentrated at the nucleation sites of the bcc phase α-Fe(Zr).

Crystallisation of amorphous alloys is extensively studied in view of the possibility of constructing nanocrystalline ferromagnetic Fe – Cu – M – Si – B alloys (M = Nb, Ta, W, Mo or Zr) with a very low coercive force and high magnetic permeability, *i.e.*, of magnetically soft materials. The magnetic

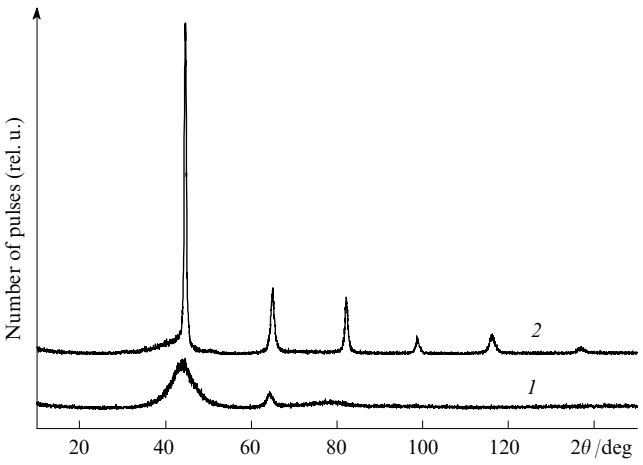



**Figure 14.** Changes in the X-ray diffraction pattern upon the transformation of the alloy $Fe_{90}Zr_7B_3$ from the amorphous (*1*) to the nanocrystalline (*2*) state.[178]
The grain size of the bcc phase α-Fe(Zr) is $\sim 10$ nm.

properties of thin films of the Ni – Fe alloy were demonstrated[179] to be improved as the effective magnetocrystalline anisotropy decreases. This can be achieved by increasing the number of grains involved in exchange interactions in thin magnetic films. In other words, a decrease in the grain size results in an increase in exchange interactions, a decrease in magnetocrystalline anisotropy and, consequently, an improvement of the properties of magnetically soft materials. More recently, this idea has been implemented in targeted crystallisation of multicomponent amorphous alloys.

Silicon-containing steels are magnetically soft materials. Initial attempts to improve the properties of these materials by crystallisation of amorphous alloys were undertaken for alloys of the Fe – Si – B system with addition of copper. However, no alloys with nanocrystalline structures could be obtained in this system. It is only after the introduction of Group IV – VII transition metals along with Cu that a nanostructure was prepared by crystallisation of this system.[180] Crystallisation of amorphous Fe – Cu – Nb – Si – B alloys at 700 – 900 K afforded an alloy with a homogeneous nanocrystalline structure. In this alloy, grains of the bcc α-Fe(Si) phase with the size of $\sim 10$ nm and copper clusters with the size of $< 1$ nm are uniformly distributed in an amorphous matrix.

Positron annihilation studies demonstrated[79] that $(Fe_3Si)_{95}Nb_5$ alloys are thermally stable due to segregation of Nb atoms at the interfaces. Due to the high melting point, niobium hinders complete recrystallisation of the alloy.

The preliminary (before crystallisation annealing) rolling deformation of amorphous Fe – Cu – Nb – Si – B alloys (or their low-temperature annealing) allows a decrease in the grain size to $\sim 5$ nm.[181]

Crystallisation of rapidly solidifying aluminium alloys Al – Cr – Ce – M (M = Fe, Co, Ni or Cu) containing 92 at.% Al gave a structure containing an amorphous phase and icosahedral aluminium-rich nanoparticles with the size of $\sim 5 - 12$ nm.[182]

## XI. Severe plastic deformation

Severe plastic deformation is a very attractive procedure for the preparation of compact nano- and submicrocrystalline materials.[19, 183 – 186] This method is based on the formation of strongly fragmented and disoriented structures with signs of a recrystallised amorphous state. Large deformations of materials can be achieved with the use of the following methods:

twisting under quasi-hydrostatic pressure, equal-channel angular pressing, rolling and three-dimensional forging. These methods consist of performing multiple intense plastic shear deformation of materials, the true logarithmic deformation ($e$) being 4–7. The use of severe plastic deformation allows not only a decrease in the average grain size but also the production of massive samples with a virtually pore-free structure, which cannot be achieved by compaction of nanopowders.

Twisting under high pressure of disc-shaped samples with the radius $R$ and the thickness $l$ creates shear deformations. The geometric shape of samples is such that the main bulk of materials is deformed under quasi-hydrostatic compression and, hence, the samples are not destroyed in spite of a high degree of deformation. The true logarithmic deformation achieved upon twisting under high pressure is calculated by the equation [183]

$$e = \ln\frac{\theta R}{l}, \tag{7}$$

where $\theta$ is the twist angle in radians. The results of numerous investigations demonstrated that after several turns, the structure of samples is disintegrated both at the periphery and in the central part so that it becomes homogeneous throughout the bulk.[19]

The most homogeneous structure is formed upon steady-state simple shear deformation. In this method, a material is pressed through two channels of equal cross-section intersecting at an angle of $2\Phi = 90-150^\circ$. The intersection plane of the channels contains a homogeneous localised simple shear deformation with an intensity of

$$\Delta\Gamma = 2\cot\Phi. \tag{8}$$

Multiple cycling treatment of a material according to this scheme provides superhigh intense deformations

$$\Gamma = N\Delta\Gamma = 2N\cot\Phi,$$

where $N$ is the number of cycles. The resulting sample exists in a homogeneous stressed deformed state, but its cross-section sizes remain unchanged. The true logarithmic deformation is calculated by the equation

$$e = \operatorname{arsh}\frac{\Gamma}{2} = \ln\left\{\frac{\Gamma}{2} + \left[\left(\frac{\Gamma}{2}\right)^2 + 1\right]^{1/2}\right\}. \tag{9}$$

It is most reasonable to use angles $2\Phi$ close to 90°, at which the maximum intensity of deformations is achieved, an increase in the contact pressure being insignificant. A grease is used to minimise contact frictions. This deformation scheme is called equal-channel angular pressing. This method was described for the first time by Segal [187] and was developed further.[188, 189]

The results of investigations of the structures and properties of submicrocrystalline materials were analysed in reviews.[19, 185, 190] Annealing of nanocrystalline materials leads to evolution of their microstructures, which can arbitrarily be divided into two steps. In the first step, annealing at a temperature equal to approximately one third of the melting point leads to stress relaxation, the transformation of the grain boundaries from the nonequilibrium to a more equilibrium state and a slight grain growth. In the second step, further increase in the annealing temperature or an increase in the annealing time cause collective recrystallisation (grain enlargement). The first annealing step can readily be observed from the results of microhardness measurements of plastically deformed materials, for example, of Cu, Pd and Ti (Fig. 15).

The severe plastic deformation was applied to obtain nano- and submicrocrystalline structures of metallic Cu,[191–193] Pd,[194–197] Fe,[198] Ni [191, 193, 199] and Co,[200] aluminium-,[184] magnesium- [201] and titanium-based [202, 203] alloys and a number of brittle compounds. Interestingly, after plastic deformation of similar strength, the grain size in brittle compounds was smaller than in metals. For example, a compact nanocrystalline sample with a grain size of ~30–40 nm was prepared for the first time [204, 205] from a coarsely dispersed nonstoichiometric powder of carbide $TiC_{0.62}$ (with a particle size of ~2–5 μm) by twisting under quasi-hydrostatic pressure.

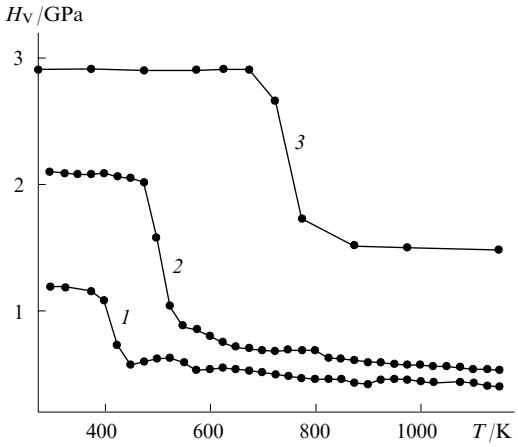



**Figure 15.** Plots of the microhardness of plastically deformed metals Cu (*1*), Pd (*2*) and Ti (*3*) *vs.* the annealing temperature.

The synthesis of nanocrystalline titanium monoxide by twisting under quasi-hydrostatic pressure of 8 GPa was documented.[206] The size of coherent scattering regions estimated from the Williamson–Hall plot was ~40 nm. In addition, it was found that the cubic lattice parameter of titanium monoxide was increased by 0.0004 nm after mechanical treatment (Fig. 16), which is indicative of a substantial change in the concentration of titanium vacancies.[206] Particular attention is given to structural vacancies in this compound, because they are responsible for the properties of the monoxide.

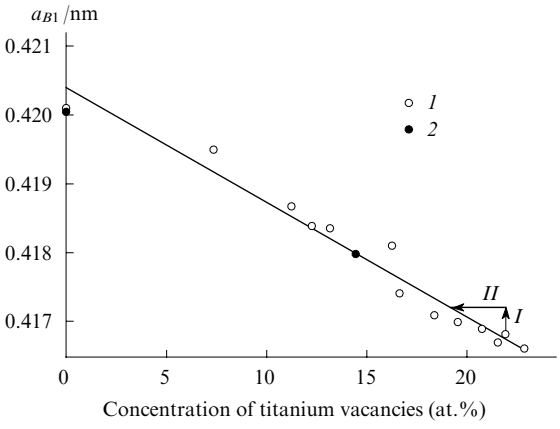



**Figure 16.** Plot of the lattice parameter of titanium monoxide $a_{B1}$ *vs.* the concentration of structural vacancies in the metal sublattice for the equilibrium state (*I*) and the stoichiometric monoxide subjected to a pressure of 8 GPa at high temperature (*2*).[206]
The increase in the lattice parameter of titanium monoxide $TiO_{1.23}$ (*I*) and the decrease in the concentration of titanium vacancies (*II*) after severe shear deformation under a pressure of 8 GPa at room temperature are indicated by arrows.

## XII. Electric explosion

Nanopowders can be prepared by electric explosion of conductors caused by passing a powerful current pulse with density of $10^4 - 10^6$ A mm$^{-2}$ and duration of $10^{-5} - 10^{-7}$ s.[207–209] For this purpose, a wire with a diameter of 0.1 – 1.0 mm is used. An electric explosion of a conductor is accompanied by a sharp change in the aggregation state of metal as a result of intense energy release and by the shock wave generation, enabling rapid (at a rate of higher than $1 \times 10^7$ K s$^{-1}$) heating of metals to high temperatures ($T > 10^4$ K). In the initial step of electric explosion, heating of conductors is accompanied by their linear expansion at a rather low rate (1 – 3 m s$^{-1}$). In the explosion step, the metal is overheated to a temperature higher than the melting point, expansion of the compound occurs at a rate of up to $5 \times 10^3$ m s$^{-1}$ and the overheated metal is explosively dispersed.[210] The pressure and temperature at the shock wave front achieve several hundreds of megapascals (thousands of atmospheres) and $\sim 10^4$ K, respectively. Condensation in a flow of rapidly expanding vapour affords very small particles. Powders with a particle size from 100 μm to 50 nm can be prepared by controlling the explosion conditions. The average particle size monotonically decreases with an increase in the current density and decrease in the pulse duration. Metal and alloy powders can be prepared by electric explosion in an inert atmosphere. Finely dispersed powders of metal oxides, nitrides and carbides or their mixtures can be prepared by intoducing additional reagents (air, a mixture of oxygen and an inert gas, nitrogen, distilled water, decane, paraffin or a technical oil) into a reactor. Copper powders with the maximum of the size distribution corresponding to $\sim 20$ nm and aluminium powders with an average particle size of $\sim 50$ nm were prepared by electric explosion at a pressure of 200 Pa.[208]

According to experimental data,[211] submicrocrystalline powders prepared by electric explosion of a wire have a very high excess energy. For example, the excess energy of aluminium powders with an average particle size of 500 – 800 nm is 100 – 200 kJ mol$^{-1}$ and of silver powders with an average particle size of $\sim 120$ nm is 40 – 80 kJ mol$^{-1}$, which is several times higher than the heat of melting of a massive substance. This excess cannot be attributed to a contribution of only the surface energy. The observed accumulation of a large excess energy by finely dispersed powders prepared by electric explosion [211] remained unexplained. It was hypothesised [212] that the excess energy is accumulated as the surface energy, internal defects and charge states. The size distribution of powders is logarithmically normal, and the maximum of distribution is in the range of 10 – 500 nm. Particles of metal and alloy powders prepared by electric explosion are spherical, whereas particles of nitride powders are faceted.

In recent years, the electroerosion method was developed for the preparation of nano- and submicrocrystalline metal and alloy powders.

## XIII. Ordering of non-stoichiometric compounds as a method for the construction of nanostructures

Group IV, V and VI transition metal carbides hold promise for the construction of nanocrystalline ceramic materials having rather high hardness, low fragility and stability against cracking. These ceramics belong to highest-melting compounds and they are inferior only to diamond and cubic boron nitride in hardness.

Group IV and V transition metal monocarbides $MC_y$ are strongly non-stoichiometric compounds.[213–215] In the disordered state, these compounds have the cubic structure $B1$ and contain up to 50% structural vacancies in the non-metal sublattice.[51, 213–220] At temperatures below 1300 K, the structure $B1$ becomes unstable, and non-stoichiometric carbides undergo first-order disorder – order phase transitions accompanied by a jumpwise change in the volume and the formation of ordered phases with complex superstructures.[213–221] Since the ordering is a diffusion process, the transformation occurs during a particular temperature-dependent period of time. Carbides are synthesised at 1400 – 1800 K, which is above the disorder – order phase transition temperatures ($T_{trans}$). Cooling of carbides to room temperature is accompanied by ordering. In the rapid cooling, ordering is not completed and non-stoichiometric carbide persists in a metastable disordered state. A difference in the lattice parameters of disordered and ordered phases gives rise to stresses, which can lead to cracking of crystallites at interfaces. Nanostructured powders of non-stoichiometric carbides can be prepared by decreasing the domain size of the ordered phase.

An idea of the nanostructure formation by atom-vacancy ordering of non-stoichiometric compounds was applied for the first time to non-stoichiometric vanadium carbide.[222] The latter was chosen for investigation because ordering in this compound is the most pronounced.[221, 223, 224] In nanocrystalline solids and nanopowders, not only bulk effects (associated with the particle size), but also surface effects (associated with the state and structure of interfaces) [9–12] play an important role. This is why particular attention was given to the surface state of compounds in the studies on physicochemical properties of vanadium carbide.[222, 225]

Particles of nanostructured powdered vanadium carbide $VC_{0.875}$ were obtained by carbothermal reduction of oxide $V_2O_5$ followed by cooling to room temperature. Vanadium carbide is nanostructured, and its nanoparticles are curved and petal-shaped. The petals are joined to each other to form a coral-like structure (Fig. 17). An electron microscopic study revealed small deviation of the nanoparticle size. Nanostructured vanadium carbide is unique because this structure has not been found earlier.

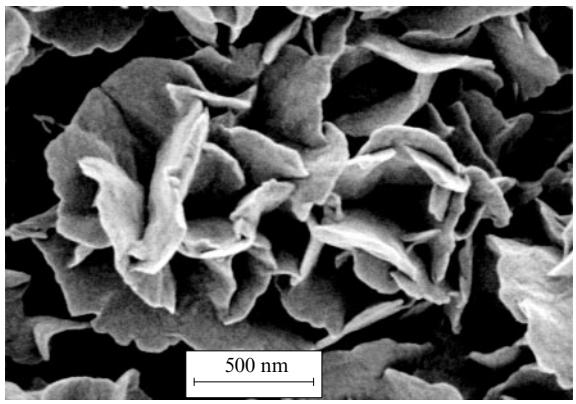



**Figure 17.** Morphology of particles of the vanadium carbide powder $VC_{0.875}$.[222]
Particles with the size of $\sim 1$ μm are two-dimensional nanocrystallites having a shape of curved petal discs with a diameter from 400 to 600 nm and thickness of $\sim 15 - 20$ nm.

The crystal structure of vanadium carbide was studied by X-ray diffraction using Cu$K\alpha_{1,2}$ radiation.[225, 226] The X-ray diffraction spectra of disordered, coarse-grained ordered and nanostructured carbide $VC_{0.875}$ are presented in Fig. 18. The X-ray diffraction pattern of a $VC_{0.875}$ nanopowder (Fig. 18 *c*) shows, along with structure reflections of the basic phase $B1$, only superstructure reflections corresponding to the cubic ordered phase $V_8C_7$ with the space group $P4_332$. The lattice parameter of the disordered phase is

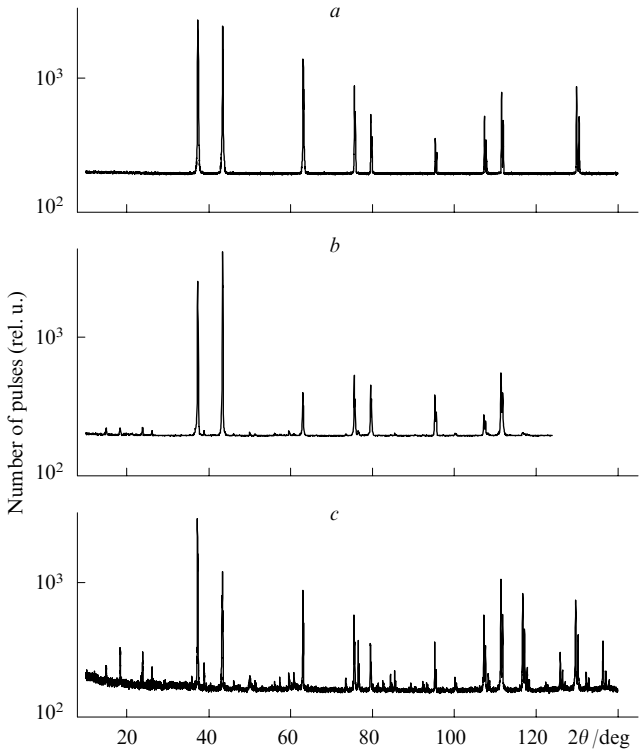



**Figure 18.** X-Ray powder diffraction patterns of disordered (*a*), ordered coarse-grained (*b*) and nanostructured carbide $VC_{0.875}$ (*c*) ($CuK\alpha_{1,2}$ radiation, the intensity is shown on the logarithmic scale; the structure reflections of the phase *B*1 are indicated).[226]
The superstructure reflections in the X-ray diffraction patterns (*b*) and (*c*) correspond to the cubic ordered phase $V_8C_7$: $a_{B1}$/nm: (*a*) 0.41638, (*b*) 0.41682, (*c*) 0.41685.

$0.8337 \pm 0.0001$ nm. The ideal $M_8C_7$-type cubic superstructure with the space group $P4_332$ has the doubled (compared to the disordered basic phase *B*1) lattice parameter.[219, 220, 224] Hence, the lattice parameter of the basic phase $a_{B1}$ of the vanadium carbide under study is 0.41685 nm. This parameter is substantially (by 0.00047 nm) larger than the lattice parameter of disordered carbide $VC_{0.875}$. Such a large difference can be observed only in the case of the maximum (or nearly maximum) degree of ordering.[217, 219, 220]

The intensity of superstructure reflections of coarsely crystalline ordered carbide $VC_{0.875}$ decreases with the increase in the diffraction angle $2\theta$ (Fig. 18 *b*), whereas the intensity of superstructure reflections of the nanopowder in the angle range $2\theta > 100^\circ$ even increases rather than decreases (Fig. 18 *c*). This fact remains unexplained.

In spite of the nanometre thickness of nanocrystallites, an analysis of X-ray reflections did not reveal their broadening. Since all atoms in the crystallite scatter coherently, the absence of broadening of X-ray lines is consistent with the presence of a rather large number of atoms in nanocrystallites, as evidenced by a large size of the latter in two other dimensions.

Electron–positron annihilation is the most efficient and sensitive method for studying defects at interfaces and on the surfaces of nanoparticles. The positron trapping by such defects as vacancies or nanopores results in an increase in the positron lifetime compared to that in defect-free materials [227] and in changes in the Doppler broadening spectra of annihilation $\gamma$ quanta.[228] The defect type can be judged from the lifetime.

The positron lifetime was measured with the use of a $VC_{0.875}$ carbide powder pre-calcined at 400 K to remove

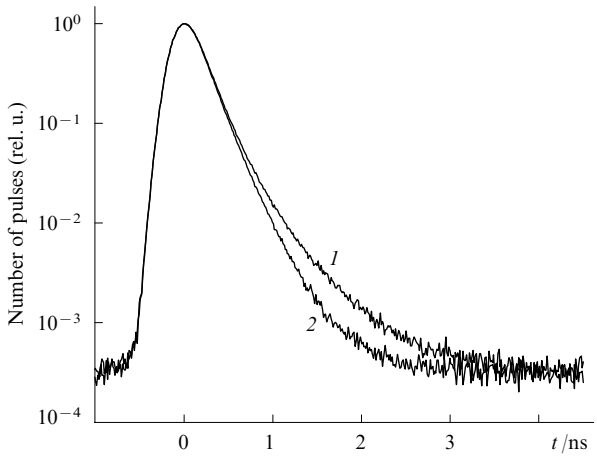



**Figure 19.** Positron lifetime spectra of nanostructured (*1*) and coarse-crystalline (*2*) powders of ordered carbide $V_8C_7$;[222]
*t* is the current time.

water.[222, 225] For comparison, the positron lifetimes were measured in a coarse-grained sintered sample of $VC_{0.875}$. The positron lifetime spectra are shown in Fig. 19. The average positron lifetime in the nanopowder is substantially longer than that in the polycrystal. The spectrum of the coarse-grained sample of vanadium carbide shows only a short-lifetime component with $157 \pm 2$ ps, which corresponds to positron annihilation of a structural vacancy in the carbon sublattice.[229, 230] The spectrum of the nanocrystalline sample contains a short-lifetime component along with a long-lifetime component with 500 ps and a relative intensity of 7%. The long-lifetime component is attributed [227] to positron annihilation in defects on the particle surface. The positron trapping by a structural vacancy is evidence of the absence of long-distance diffusion of positrons. In this case, the intensities of the components are proportional to the volume fractions of phases containing different types of defects. Thus, the relative intensity of the long-lifetime component is consistent with the volume fraction of the surface

$$\Delta V_{\text{surf}} = \delta \frac{S}{V}$$

in the nanopowder. The surface layer was estimated to have thickness $\delta = 0.5-0.7$ nm or 3–4 atomic monolayers. The results of determination of the positron lifetime show that the inner part of vanadium carbide nanocrystallites contains only non-metal structural vacancies and the surface layer involves vacancy agglomerates as defects.

The observed morphology of the nanocrystalline powder of non-stoichiometric vanadium carbide may be a consequence of grain cracking at the interfaces between the disordered and ordered phases. Actually, high-temperature X-ray diffraction measurements demonstrated [221] that a jumpwisee increase in the lattice parameter of the fcc sublattice by 0.0004 nm occurs at $1413 \pm 20$ K as a result of the disorder–order phase transition. The domain size of the ordered phase is $\sim$20 nm. It was shown [223] that ordering occurs according to the mechanism of the first-order phase transition at $1368 \pm 12$ K. At 300 K, the parameter $a_{B1}$ of the basic crystal lattice of quenched disordered carbide $VC_{0.875}$ is 0.0002 nm smaller than that of ordered carbide with the same carbon content. The difference between the volumes of the disordered and ordered phases is responsible for the appearance of stresses and subsequent cracking at the interfaces.

The nanostructure formation can proceed according to another mechanism. Unlike the above-considered mechanism associated with the presence of domains of disordered and ordered phases, the mechanism under discussion involves the formation of antiphase domains of the ordered phase. The first-order disorder – order phase transition affords domains of the ordered phase between which stresses occur due to a mismatch of the atomic structures of antiphase domains. In due course, stresses lead to cracking of grains of the initial disordered phase at the antiphase domain boundaries of the ordered phase.

According to this mechanism, the nanostructure formation of a non-stoichiometric $VC_{0.875}$ powder (see Fig. 17) can be attributed to the $VC_{0.875} \rightarrow V_8C_7$ phase transition. Nanocrystallites of ordered non-stoichiometric vanadium carbide are formed as curved discs with a diameter of $< 600$ nm and thickness of 15 – 20 nm through cracking of particles with the size of up to 1 μm. The inner part of nanocrystallites consists of ordered carbide $V_8C_7$ with a high degree of long-range order and a negligibly small amount of dissolved oxygen. The surface layer of nanocrystallites with a thickness of 0.5 – 0.7 nm contains chemisorbed oxygen and a large amount of vacancy agglomerates, *i.e.*, has a loose structure.

The ordering allows the nanostructure formation in compact samples of non-stoichiometric compounds.

The structures of annealed and quenched compact samples of $VC_{0.875}$ were studied by X-ray diffraction. After both annealing and quenching, the X-ray diffraction spectra contain, along with the structure reflections, weak additional reflections (Fig. 20). The positions of additional reflections correspond to superstructure reflections and are assigned to the ordered cubic phase $V_8C_7$ with the space group $P4_332$. The superstructure reflections for annealed and quenched samples are similar in the integral intensity but strongly differ in the width.

According to the equilibrium phase diagram of the V – C system,[231] the ordered $V_8C_7$ phase is formed after the disorder – order phase transition at 1380 K; the experimental phase transition temperature is $1413 \pm 20$ K.[221] Rapid cooling from 1420 and 1500 to 300 K could result in quenching of non-stoichiometric vanadium carbide $VC_{0.875}$ and its retention in a metastable state. However, even quenching from 1500 K gives rise to the ordered $V_8C_7$ phase, the relative intensities of superstructure reflections being approximately equal to those for samples obtained after quenching from 1420 K or annealing at 1370 K (see Fig. 20).

As a consequence of ordering, each grain of the basic disordered phase is divided into domains of an ordered phase. The degree of ordering in domains is high, whereas the mutual spatial arrangement of domains is random to a degree allowed by the ratio between the structures of the ordered phase and the disordered matrix. X-Ray diffraction studies showed that the width of structure reflections is independent of the conditions of thermal treatment of compact $VC_{0.875}$ samples. Hence, the grain size of the basic phase presumably remains unchanged upon ordering. However, the superstructure lines are substantially broadened, which can be attributed to a small domain size of the ordered phase formed under different conditions of thermal treatment. Since the width of reflections depends on the domain size and the resolution of the instrument used for measurements, the domain size can be determined by measuring the broadening. Let us assume that the deformation broadening is absent in the first approximation and the observed broadening $\beta$ is associated only with a small domain size, *i.e.*, $\beta = \beta_s$. In this case, the broadening

$$\beta_s(2\theta) \equiv 2\beta_s(\theta),$$

measured in radians is related to the average domain size $\langle D \rangle$ by the Scherrer equation.

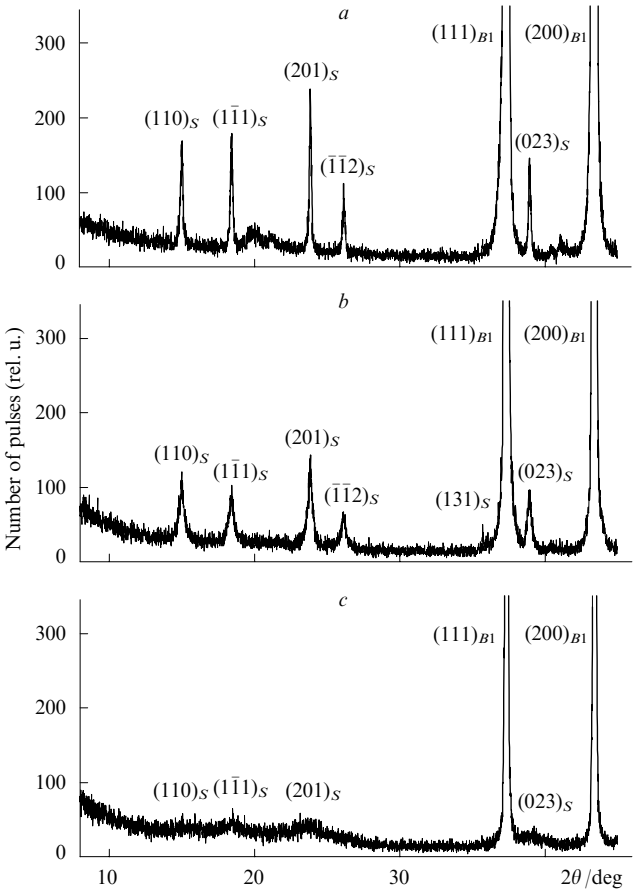



**Figure 20.** X-Ray diffraction patterns of compact samples of $VC_{0.875}$ prepared by hot pressing and subjected to additional thermal treatment ($CuK\alpha_{1,2}$ radiation, the structure reflections of the phase $B1$ and the superstructure reflections of the phase $V_8C_7$ are indicated).[226]
(*a*) Annealing at 1370 K for 2 h followed by slow cooling to 300 K; (*b*) quenching from 1420 to 300 K at a cooling rate of 100 K $s^{-1}$; (*c*) quenching from 1500 to 300 K at a cooling rate of 100 K $s^{-1}$; all X-ray diffraction patterns show superstructure reflections of the ordered cubic phase of $V_8C_7$; the most broadened superstructure reflections are seen in the X-ray diffraction pattern of a sample of $VC_{0.875}$ quenched from 1500 K.

The largest broadening of superstructure reflections is observed for a sample quenched from 1500 K; the least broadening, for a sample annealed at 1370 K. This suggests that the ordered phase in the former sample has the minimum domain size. Annealed vanadium carbide is characterised by the maximum domain size because annealing followed by slow cooling provide more favourable conditions for the domain growth. The determination of the broadening $\beta_s$ and an estimation of the average domain size of the ordered phase gave the following results: the domain size in annealed samples (see Fig. 20 *a*) is $127 \pm 10$ nm with 95% confidence probability; in samples prepared by quenching from 1420 K (see Fig. 20 *b*) and 1500 K (see Fig. 20 *c*), the domain sizes are $60 \pm 9$ and $18 \pm 12$ nm, respectively, with the same confidence probability.

Thus, annealing and quenching of compact samples of non-stoichiometric carbide $VC_{0.875}$ from $T_{trans} \pm 100$ K are accompanied by the nanostructure formation, the nanostructure being composed of domains of the ordered phase. The higher the annealing (quenching) temperature or the higher the cooling rate, the smaller the domain size. The nanostructure

formation in compact non-stoichiometric $VC_{0.875}$ is associated with the $VC_{0.875} \rightarrow V_8C_7$ phase transition.

The disorder – order transitions accompanied by a change in the volume can be used for the formation of the nanostructured state not only in strongly non-stoichiometric compounds, but also in substitution solid solutions. It was suggested [232] that polymorphic phase transitions would be used for the nanostructure formation in compact compounds.

## XIV. Properties and application of nanomaterials

The properties of nanomaterials are substantially different from those of other materials because the properties of nanoparticles differ from those of large particles. In addition, nanoparticles interact with each other in a fashion different from that of large particles because the distances at which interactions occur in electron, phonon and magnon subsystems are comparable with the sizes of nanoparticles. The properties of the latter differ from those of atoms or associations of atoms but are still different from the properties of compounds consisting of a large number of atoms (solid materials). In addition, nanoparticles have no thermodynamically equilibrium atomic-molecular structure due to which their properties can assume a number of values for the same particle size depending on the conditions of synthesis and the temperature prehistory.

Due to high energy of nanoparticles, their structures are not necessarily equilibrium. Accumulation of experimental data on this problem is presently underway. For example, it was demonstrated [21] that the structure of cadmium sulfide nanoparticles differs from those of this compound in the wurtzite (equilibrium under normal conditions) and sphalerite phases. The atomic structure of nanoparticles is actually disordered to a large degree although the short-range order is almost completely retained. The atomic structure of cadmium sulfide nanoparticles can be represented as disordered superimposed close-packed planes consisting of cadmium and sulfur atoms. The three-dimensional model of CdS nanoparticles containing 3038 cadmium atoms with a disordered structure of the metal sublattice (*ACABCBC*) was described.[21] The particle height ($h$) is 2.3 nm, the distance ($d$) between the lateral faces is 5.7 nm, and the aspect ratio of the particle sizes $d/h \sim 2.5$. Calculations by the Debye equation demonstrated a good agreement between X-ray diffraction spectra and experimental data. A lattice with the space group $P6/mmm$ can be considered as an average crystal lattice of the cadmium sulfide nanophase (Fig. 21).

The properties of isolated nanoparticles along with a disorder are also determined to a large extent by the contribution of the surface layer. For a spherical particle with a diameter $D$ and surface layer thickness $\delta$, the surface layer fraction ($\Delta V$) in the total particle bulk ($V$) is

$$\frac{\Delta V}{V} = \left[\frac{\pi}{6}D^3 - \frac{\pi}{6}(D-2\delta)^3\right]\left(\frac{\pi}{6}D^3\right)^{-1} \approx \frac{6\delta}{D}.$$

If the surface layer thickness is equal to 3–4 atomic monolayers (0.5–1.5 nm) and the average nanocrystallite size is 10–20 nm, up to 50% atoms of a substance are located in the surface layer.[222] Hence, the properties of nanoparticles are determined by their large specific surface area and the strong effect of the near-surface atoms. The coordination of these atoms and their interatomic distances differ from those of atoms located far from the surface. In many cases, the near-surface atoms have high energy, resulting in a decrease in the temperature of chemical reactions between nanoparticles, and the reaction intensity increases as a consequence of a large specific surface area of nanoparticles.

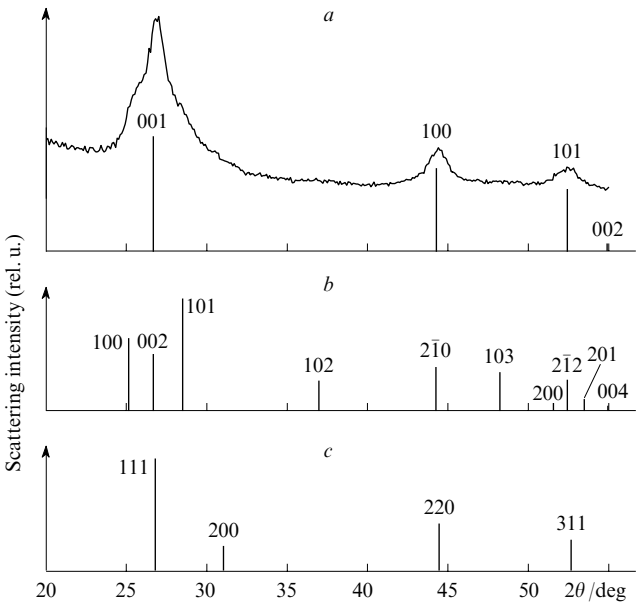



**Figure 21.** The experimental X-ray diffraction spectrum of a CdS powder (*a*) and linear spectra of different structures.[21]
(*a*) The linear spectrum of a disordered structure, the space group of the average lattice is $P6/mmm$; (*b*) the linear spectrum of the wurtzite structure $B4$, the space group $P6_3mc$; (*c*) the linear spectrum of the sphalerite structure $B3$, the space group $F\bar{4}3m$.

Interactions between nanoparticles differ from those between microparticles. The interfaces between nanoparticles make a large contribution to the properties of assemblies of nanoparticles. For example, the structure of high-angle interfaces between nanoparticles often determines the mechanical properties of nanomaterials. The electric and magnetic properties depend to a large degree on the ratio between the coherence lengths of electron, phonon and magnon interactions and the distances between the centres of nanoparticles. In many cases, the nicrostructures of nanomaterials are determined by interactions between nanoparticles. For example, the van der Waals forces are responsible for the mutual arrangement of nanoparticles. The interactions result in self-organisation of nanoparticles in nanomaterials.[17, 18, 80, 87]

In studies of compact nanomaterials, solid materials are considered as assemblies of interacting grain-boundary defects. For example, the symmetry properties of polycrystals in relation to changes in the characteristic scale of structural heterogeneity, *i.e.*, the grain size, are analysed [233] using the calibration field theory,[234, 235] which was developed for the description of the structural and physical properties of materials with defects. An increase in the grain size to several nanometres was demonstrated [233] to lead to the topological transition from isolated waves of orientation shear instability, which are characteristic of the usual polycrystalline state, to spatially periodic defect structures. This topological transition in an assembly of grain-boundary defects is accompanied by a sharp change in the connectivity characteristics and scaling parameters. The validity of this approach is associated with the fact that the concentration of defects in nanomaterials is so high that interactions occur between the defects. For a few nanomaterials in which the concentration of defects is low the application of the calibration field theory is unjustified.

The use of the size effects is convenient for analysing changes in different properties of solids. Actually, there is abundant evidence of the influence of the nanostate on the magnetic properties of ferromagnets, the Curie temperature, coercive forces, the saturation magnetisation and the magnetic

susceptibility of weak para- and diamagnets, the memory effects on the elastic properties of metals, substantial changes in the heat capacity and hardness, changes in the optical and luminescence characteristics of semiconductors and the plasticity of boride, carbide, nitride and oxide materials, which are rather brittle in the usual coarse-grained state.

It has long been known that the properties of small particles differ from those of massive substances. This fact is used in industry. Aerosols, colouring pigments and colouration of glass melts by colloidal metal particles for the preparation of colour glasses can be referred to as examples. Suspensions of metal nanoparticles (generally iron or its alloys) with the size of 30 nm and larger are used as engine oil additives for restoring worn-out details of internal combustion engines directly during operation. Small particles and nanometre-sized elements are used in the production of different aircraft materials, for example, of radio-absorbing ceramics the matrices of which contain randomly distributed metal nanoparticles.

Polymerised rhombohedral fullerene $Rh-C_{60}$ has the Curie temperature of 500 K and the hysteresis curve typical of ferromagnets.[236] A light magnet operating at room temperature can be constructed from this nanomaterial. In fullerene crystals, $C_{60}$ molecules are linked to each other by weak van der Waals forces, whereas the presence of nitrogen atoms in the fullerene-like nanomaterial $C_{48}N_{12}$ is responsible for the appearance of strong covalent bonds. Hence, the latter material can be employed when a combination of strength and elasticity is required.

Carbon nanotubes show high mechanical stability. Hence, they can be used for the construction of high-strength composites. It is expected that nanotubes will find application in the construction of various mechanical nanodevices.[237] Carbon nanotubes are already used as nanoindenters in microhardness measurements and as probes in atomic-force microscopes.[238] Carbon nanotubes exhibit semiconductivity or metal conductivity depending on the arrangement of carbon atoms in their walls. Due to this fact, these nanotubes are used as conducting elements in nanoelectronics.

Various structures having different properties can be prepared by connecting carbon nanotubes. The synthesis of such structures is of importance for application in electronic technique. Carbon nanotube T-junctions[239] can operate as contact devices. Due to a defect structure, Y-nanotubes[240] allow current to pass in one direction at the junction of teeth and operate as diodes.[241] The stem of Y-nanotubes has a diameter of $\sim$60 nm. The diameter of branches is $\sim$40 nm. If a controlling voltage is applied to one tooth of an Y-nanotube, the latter will operate as a current stabiliser. The possibility of controlling the current holds promise for the use of Y-nanotubes in nanoelectronics.

Bundles of multilayer carbon nanotubes with a diameter of 20–30 nm that were grown on a substrate coated with a $SiO_2$ layer, can find application in next generation integrated microcircuits and in microelectromechanical devices.[242] Nanotubes can be used as atomic-molecular pumps for depositing individual molecules, atoms or ions onto the surface.[243] The results of investigations and applications of various carbon and noncarbon nanotubes were summarised in reviews.[244–246]

Catalysis of chemical reactions is an important field of application of metal, alloy and semiconductor nanoparticles.

High catalytic activity of small particles is attributed to the electronic effect. Actually, the number of atoms in an isolated metal particle is small and, consequently, the distance between the energy levels $\delta \approx E_F/N$ ($E_F$ is the Fermi energy and $N$ is the number of atoms in the particle) is comparable with the energy $kT$. In the limit, when $\delta > kT$, the energy levels are discrete and the particle loses metallic properties. Nanoparticles begin to exhibit catalytic activity at $\delta \approx kT$. For metals, the Fermi energy is 10 eV. At $\sim$300 K, $\delta$ is 0.025 eV and, hence, $N \approx 400$. The particle consisting of 400 atoms has a diameter of $\sim$2 nm.

As a rule, nanoparticles exhibit catalytic activity in a very narrow size range. For example, rhodium catalysts, which are synthesised by decomposition of the $Rh_6(CO)_{16}$ clusters deposited on the surface of dispersed silica, catalyse benzene hydrogenation only if the particle size is 1.5–1.8 nm, *i.e.*, only $Rh_{12}$ particles are actually catalytically active in this reaction. High selectivity of the catalytic action is typical also of nanoparticles of such popular catalysts as palladium and platinum. For example, a study of ethylene hydrogenation at 520 K under a hydrogen pressure of 1 atm catalysed by platinum deposited on $SiO_2$ or $Al_2O_3$ revealed a pronounced maximum of the reaction rate corresponding to the platinum nanoparticle size of $\sim$0.6 nm. Such a high sensitivity of the catalytic action to the size of small particles demonstrates the importance of the development of selective procedures for the preparation of nanoparticles with an accuracy to one atom. Materials characterised by a very narrow size distribution of nanoparticles are required not only for catalysis, but also for nanoelectronics.

A detailed analysis of the size effect of small metal and alloy particles deposited on a support was performed;[247] the reviews[248–250] deal with catalysis involving metal alloys and palladium.

A new field of catalysis on nanoparticles, *viz.*, photocatalysis with the use of semiconductor particles and nanostructured films, holds promise for purification of water from organic contaminants by photocatalytic oxidation and mineralisation. For example, colloidal solutions of semiconducting oxide and sulfide nanoparticles (without deposition on a substrate) and the nanocrystalline heterostructures ZnS/CdSe, HgS/CdS, ZnS/ZnO and $TiO_2/SnO_2$ are used in the photocatalytic synthesis and destruction of organic compounds as well as in decomposition of water.[98–101]

Polymeric composites containing metal nanoparticles are used as conducting film composite materials, the possible amount of the filling agent in the matrix being as high as 90 vol.%. Hybrid metal–polymer composites can be synthesised by the nanoparticle formation in a polymeric matrix.[251,252] Coloured light guides for computer techniques are produced by introducing metal ions into polymeric fibres. The optical properties of polymers filled with metal, alloy or semiconductor (CdS, CdSe, InP or InAs) nanoparticles are of interest. Such polymers are easily subjected to mechanical treatment and can be used for the preparation of films. Hence, such polymers hold promise as optical elements and light filters.

Multilayer nanostructures are widely applied in the microelectronic device manufacturing. Layered inhomogeneous nanostructures, *viz.*, superlattices consisting of alternating solid superthin layers (with a thickness from several to one hundred crystal lattice parameters or $\sim$1–50 nm) of two different compounds, can be referred to as an example. This crystal structure contains, along with a usual lattice of periodically arranged atoms, a superlattice consisting of repeated layers with different compositions. Since the nanolayer thickness is comparable with the de Broglie wavelength of the electron, the quantum size effect is manifested in the electronic properties of superlattices. The use of this effect in multilayer nanostructures allows the design of fast-operating electronic devices with a high information capacity. The double-barrier diode AlAs/GaAs/AlAs consisting of a gallium arsenide layer with a thickness of 4–6 nm, which is located between two aluminium arsenide layers with a thickness of 1.5–2.5 nm, is an example of the simplest electronic devices.

Magnetic nanostructures showing giant magnetoresistance are of interest. These nanostructures are multilayer films

composed of alternating layers of ferromagnetic and non-magnetic metals. For example, ferromagnetic Co–Ni–Cu layers and non-magnetic Cu layers alternate in the Co–Ni–Cu/Cu nanostructure. The layer thickness is approximately equal to the electron free path, *i.e.*, to several tens of nanometres. The magnetic configuration of multilayer nanostructures can be changed by varying the external magnetic field intensity from 0 to a particular value $H$ so that the conductivity varies in a very broad range. These films can be used as magnetic field detectors. In the nanostructure under consideration, the largest giant magnetoresistance was achieved for very thin ($\sim$0.7 nm) copper layers.

In modern microcircuits produced on a large scale, $\sim$1000 electrons are required for transistor switching on/off. Due to miniaturisation of microcircuits, the number of required electrons would be decreased to ten in the nearest future.[253] Besides, studies aimed at constructing single-electron transistors are presently underway.[254]

A device consisting of two condenser plates and a metallised ball hanged between these plates was developed. Under the action of direct-current voltage applied to the plates, the ball swings and transfers the charge. In the nanoversion, such nanopendula (or electronic shuttles) can operate at a frequency of $\sim$100 MHz and transfer individual electrons.[16, 255] Such devices would be expected to serve as elements of quantum computers or current interrupters.

Semiconducting heterostructures consisting of two or more different materials are of particular interest. In these heterostructures, a transition layer, *viz.*, the interface between two materials, plays an important role. Moreover, the interface in semiconducting heterostructures can be used as a technical device.[256]

Molecular-beam and liquid-phase epitaxies allow the growth of heterostructures with a sharp interface. Two interfaces can be located so close to each other that the quantum size effects become to play the key role. Such structures are called quantum wells. In quantum wells, the thickness of the medium layer is several tens of nanometres, resulting in electron level splitting due to the size quantisation effect. This effect, which is manifested as a characteristic stepwise structure of optical absorption spectra of the semiconducting heterostructure GaAs–AlGaAs with a hyperfine GaAs layer (a quantum well), was observed for the first time in 1974.[257] In this study, it was also found that characteristic energies are shifted as the thickness of the quantum well (a GaAs layer) decreases. In quantum wells, superlattices and other structures with very thin layers, large deformations are not necessarily accompanied by the appearance of dislocations and, hence, correspondence of the lattice parameters is not required.[258] The fundamental characteristics of semiconducting crystals, such as the gap width, the effective masses and the charge carrier mobility, can be controlled with the use of heterostructures, particularly double structures, including quantum wells, quantum wires and quantum dots.

In three-dimensional semiconductors, the density of states $N(E)$ is a continuous function. A decrease in the dimensionality of a semiconductor results in a change in the energy spectrum from continuous to discrete due to its splitting (Fig. 22). The quantum well is a two-dimensional structure in which the charge carrier motion is restricted in the direction perpendicular to the layers, but the charge carriers can freely move in the plane of the layers. In quantum wires, the charge carrier motion is limited in two directions and the charge carriers freely move only along the wire axis. Quantum dots are quasi-zero-dimensional ('0'D) structures. In such structures, the charge carrier motion is limited in all three directions and these structures are characterised by completely discrete energy spectra.

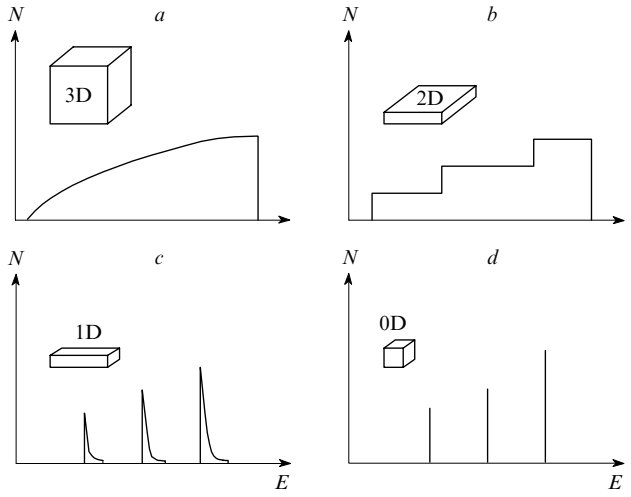



**Figure 22.** The density of states of $N$ charge carriers as a function of the dimensionality of the semiconductor.[12]
(*a*) A three-dimensional semiconductor, $dN/dE \sim E^{-1/2}$; (*b*) a quantum well, $dN/dE \sim$ const; (*c*) a quantum wire, $dN/dE \sim E^{1/2}$; (*d*) a quantum dot, $dN/dE \sim \delta(E)$.

The sizes of quantum dots obtained by molecular-beam epitaxy and lithography vary from 100 to 10 nm; smaller quantum dots (1–10 nm) the surface of which is protected by organic molecules preventing particle aggregation can be prepared by methods of colloid chemistry.[259]

Only nanotechnologies allow a decrease in the size of elements of electronic devices to several nanometres with the use of quantum dots. Time instability of nanostructures at high temperatures is a practical problem to be solved in the construction of quantum dots. Stability of quantum dots is determined by quantum jumps or diffusion of small amounts of atoms, which occur very rapidly on the surface and at interfaces of quantum electronic elements. As a result, destruction of elements or even their migration on a substrate is observed at room temperature.[260] The problem of stability of nanoelectronic circuits can be solved with the use of multicomponent materials including metal oxides, carbides and nitrides. These compounds have high melting points and low diffusion mobility of atoms and, consequently, show high thermal and time stability.

Special lenses and mirrors with multilayer coatings of alternating thin layers of elements with higher and lower densities (for example, of tungsten and carbon, molybdenum and carbon or nickel and carbon) are used in X-ray and UV optics. Two layers have thicknesses of $\sim$1 nm; the layers should be smooth at the atomic level. Multilayer X-ray lenses and mirrors are required in X-ray lithography, which is one of the fields of nanotechnology, and in astrophysical studies. The formation of X-ray mirrors was described in sufficient detail;[261] this study dealt with multilayer Ni/C nanostructures with a period of $\sim$4 nm. The Fresnel zone plates with a minimum zone width of $\sim$100 nm and diffraction lattices with a period of $<$100 nm are yet other optical devices with nanometre-sized elements intended for use in X-ray diffraction microscopy.

Heterostructures F/S are formed by alternating nanolayers of a ferromagnet (F) and a superconductor (S). Ferromagnetic interlayers of F are generally constructed of Fe, Co, Gd or Ni the Curie temperatures of which are higher than the superconducting transition temperature of metals (Nb, Pb or V) that form an S layer. Experimental studies of such heterostructures were initiated by Hauser *et al.*[262] The construction of F/S-type

superlattices can be performed with the use of molecular-beam epitaxy, electron-beam coating or magnetron spraying at direct current.[263] It should be noted that F/S-type heterostructures with layers of atomic thickness can be applied in next generation electronics as logical elements and superconducting current switches.[264, 265] In this case, the superconductivity can be controlled with a weak external magnetic field.[266] The properties of multilayer F/S systems including the superconducting transition temperature depend on the thicknesses of the ferromagnetic and superconducting layers. The thickness of a ferromagnetic layer is generally $< 1$ nm, and the thickness of a superconducting layer varies from 10 to $40-50$ nm.[266] In F/S heterostructures, the superconducting transition temperature ($T_c$) not only monotonically decreases but also oscillates as the thickness of the F layer increases. For example, an increase in the thickness of the iron layer in the three-layer system Fe/Nb/Fe from 0.1 to 0.8 nm initially leads to a lowering of $T_c$ from 7 to 4.5 K. Then the temperature rises to 5 K as the layer thickness increases to $1.0-1.2$ nm followed by a decrease in the temperature to $3.2-3.4$ K as the thickness further increases to 3 nm. In F/S heterostructures, metal and alloy ($Nb_xTi_{1-x}$/Co or V/$Fe_xV_{1-x}$) layers can alternate with each other. Superconductor/ferromagnetic semiconductor (for example, NbN/EuO/Pb or NbN/EuS/Pb) heterostructures with the Josefsson tunnel transition[267] are also of interest. The layer thickness of the ferromagnetic superconductor (EuO, EuS) in these heterostructures is $10-50$ nm and the thickness of superconducting layers is $> 200$ nm.

Ceramic nanomaterials are widely used for the production of components operating at high temperatures, under non-uniform thermal stresses and in corrosive media. Due to superplasticity, these nanomaterials can be used for the preparation of complex-configuration products with highly precise dimensions, in particular, for aerospace technique. Due to biocompatibility and high stability, hydroxylapatite-based nanoceramics are applied in orthopedy for the production of artificial joints and in dental surgery for the production of dental prostheses. Nanocrystalline ferromagnetic alloys Fe–Cu–M–Si–B (M is a Group IV–VI transition metal) have found use as soft magnetic materials for transformers with a very low coercive force and high magnetic permeability.

A method for the manufacture of a detonation diamond nanopowder is implemented in Russian industry. As a result of high pressure and temperature developed during explosion in special chambers, nanodiamond is synthesised from carbon-containing explosives catalysed by particles and metal vapour from ammunition shells.

Ultrasonic pressing of nanopowders is particularly efficient in the construction of complex-shaped articles such as sockets, conical gears, helices, *etc*.[268] The resulting ceramic articles have homogeneous microstructure and density.

The hydrothermal synthesis belonging to 'mild chemistry' methods holds promise for the preparation of nanoceramics. The synthesis proceeds at high temperature and pressure. Oxide nanoceramic materials, for example, $TiO_2$, $ZrO_2$ and $HfO_2$,[269] including nanorods can be obtained by this method.[270] Nanocrystalline titanium, zirconium and hafnium dioxide powders and composites on their basis have found use as catalysts, gas sensors, dielectric ceramics, dyes, solid electrolytes, diffusion barriers and optical coatings. The development of the hydrothermal synthesis would be expected to expand the field of application of oxide nanoceramics.

To summarise, the analysis of the scope of modern nanotechnologies and prospects of application of different classes of nanostructured materials shows the topicality of the development of nanoindustry.

## XV. Conclusion

Studies performed in the last decades provided a deeper insight into the mechanisms of size effects. Emphasis has long been placed on nanoparticles the properties of which are intermediate between those of isolated atoms and polycrystalline solids. The development of methods for the production of compact nanomaterials composed of nanometre-sized building blocks enabled researchers to investigate the properties of solids in the nanostructured state. Nowadays, the following methods are mainly used for the preparation of compact nanomaterials: compaction of isolated nanoclusters, which are obtained by evaporation and condensation, precipitation from solutions or decomposition of precursors, crystallisation of amorphous alloys, severe plastic deformation and ordering of strongly non-stoichiometric compounds and solid solutions. Each method has advantages and drawbacks, and neither is universal.

For a theoretical interpretation of experimental results obtained in studies of isolated nanoparticles and compact nanomaterials, the separation of the surface (associated with interfaces) and bulk (associated with particles sizes) effects is of considerable importance. Nowadays, this problem is far from being solved.

Nanomaterials are characterised by exceptionally high diffusion mobility of atoms along the grain boundaries. This mobility is $5-6$ orders of magnitude higher than that in usual polycrystals. However, the mechanisms of diffusion processes in nanomaterials are far from being completely understood, and different explanations of these processes were provided in the literature. The microstructure of nanocrystals, *i.e*., the structure of interfaces and the atomic density, and the influence of nanopores and the free volume on the properties of nanocrystals are still debated.

The above-considered data suggest that new nanomaterials stable at high temperature will be constructed based on multicomponent systems with the use of refractory metals and compounds. Metal oxides, nitrides and carbides with high melting points and thermal stability will be of particular importance in future nanotechnologies. These compounds will find application as components of nanocrystalline materials.The construction of stable-operating systems, which retain their properties throughout the service life, becomes possible with the use of the above-mentioned compounds.

Studies in the field of nanotechnologies and investigations of the nanostate of substances should provide the basis for a new interdisciplinary area of knowledge based on fundamental laws of physics, chemistry and biology.[271]

I thank A I Gusev, N S Kozhevnikova, A A Valeeva, A S Kurlov, A S Vorokh, S Z Nazarova, O V Makarova, V A Moldaver, R R Mulyukov, S I Sadovnikov (Russia), H-E Schaefer, A Magerl, F Hergert (Germany), R Würschum, W Sprengel (Austria), S Van den Berghe, A Leenaers, W van Renterghem (Belgium) and K Reimann (the Netherlands) for collaboration in the synthesis and investigation of nanomaterials.

## References

1. H Gleiter *Nanostruct. Mater.* **1** 1 (1992)
2. H-E Schaefer *Mechanical Properties and Deformation Behaviour of Materials Having Ultrafine Microstructure* (Eds M A Nastasi, D M Parkin, H Gleiter) (Dordrecht: Kluwer Academic, 1993) p. 81
3. R W Siegel *J. Phys. Chem. Solids* **55** 1097 (1994)

4. I D Morokhov, L I Trusov, S P Chizhik *Ul'tradispersnye Metallicheskie Sredy* (Ultradispersed Metallic Media) (Moscow: Atomizdat, 1977)
5. A I Gusev *Usp. Fiz. Nauk* **168** 55 (1998) [*Physics-Uspekhi* **41** 49 (1998)]
6. Yu I Petrov *Fizika Malykh Chastits* (The Physics of Small Particles) (Moscow: Nauka, 1982)
7. L N Larikov *Metallofizika* **14** (1) 3 (1992)
8. R A Andrievskii *Usp. Khim.* **63** 431 (1994) [*Russ. Chem. Rev.* **63** 411 (1994)]
9. A I Gusev *Nanokristallicheskie Materialy: Metody Polucheniya i Svoistva* (Nanocrystalline Materials: Methods of Production and Properties) (Ekaterinburg: Urals Branch of Russian Academy of Sciences, 1998)
10. *Nanomaterials: Synthesis, Properties and Applications* (Eds A S Edelstein, R C Cammarata) (Baltimore: Johns Hopkins University, 1998)
11. A I Gusev, A A Rempel *Nanokristallicheskie Materialy* (Nanocrystalline Materials) (Moscow: Fizmatlit, 2000)
12. A I Gusev, A A Rempel *Nanocrystalline Materials* (Cambridge: Cambridge International Science Publ., 2004)
13. K E Drexler *Nanosystems: Molecular Machinery, Manufacturing and Computation* (New York: Wiley, 1992)
14. A ten Wolde *Nanotechnology: Towards a Molecular Construction Kit* (Boston: New World Ventures, 1998)
15. *Nanostructured Materials* (Ed. J Yi-Ru Ying) (New York: Academic Press, 2001)
16. A L Buchachenko *Usp. Khim.* **72** 419 (2003) [*Russ. Chem. Rev.* **72** 375 (2003)]
17. Yu D Tretyakov *Usp. Khim.* **72** 731 (2003) [*Russ. Chem. Rev.* **72** 651 (2003)]
18. V I Roldugin *Usp. Khim.* **73** 123 (2004) [*Russ. Chem. Rev.* **73** 115 (2004)]
19. R Z Valiev, I V Aleksandrov *Nanostrukturnye Materialy, Poluchennye Intensivnoi Plasticheskoi Deformatsiei* (Nanostructured Materials, Production by Intensive Plastic Deformation) (Moscow: Logos, 2000)
20. A I Gusev *Nanomaterialy, Nanostruktury, Nanotekhnologii* (Nanomaterials, Nanostructures and Nanotechnologies) (Moscow: Fizmatlit, 2005)
21. A S Vorokh, A A Rempel *Fiz. Tv. Tela* **49** 143 (2007) [a]
22. V Kohlschütter, C Ehlers *Z. Elektrochem.* **18** 373 (1912)
23. L Harris, D Jeffries, B M Siegel *J. Appl. Phys.* **19** 791 (1948)
24. M Ya Gen, M S Ziskin, Yu I Petrov *Dokl. Akad. Nauk SSSR* **127** 366 (1959) [b]
25. V Tikhomirov, A Lidov *Zh. Russ. Fiz.-khim. O-va* **15** 421 (1883)
26. M Ya Gen, Yu I Petrov *Usp. Khim.* **38** 2249 (1969) [*Russ. Chem. Rev.* **38** 1007 (1969)]
27. B M Smirnov *Usp. Fiz. Nauk* **162** 119 (1992) [*Physics Uspekhi* **35** 37 (1992)]
28. Yu I Petrov, E A Shafranovskii *Izv. Akad. Nauk, Ser. Fiz.* **64** 1548 (2000) [c]
29. V I Vladimirov, A E Romanov *Disklinatsii v Kristallakh* (Disclinations in Crystals) (Leningrad: Nauka, 1986)
30. B M Bulakh *Rost Kristallov* (Crystal Growth) (Moscow: Nauka, 1974) Vol. 10, p. 98
31. B M Bulakh, N N Sheftal' *Rost Kristallov* (Crystals Growth) (Moscow: Nauka, 1974) Vol. 10, p. 115
32. J Muhlbuch, E Recknagel, K Sattler *Surf. Sci.* **106** 188 (1981)
33. B V Deryagin, D V Fedoseev *Rost Almaza i Grafita iz Gazovoi Fazy* (Diamond and Graphite Growth from the Gas Phase) (Moscow: Nauka, 1977)
34. A R Badzian, R C de Vries *Mater. Res. Bull.* **23** 385 (1988)
35. D V Fedoseev, Yu N Tolmachev, I G Varshavskaya *Dokl. Akad. Nauk* **349** 212 (1996) [d]
36. B Gunther, A Kampmann *Nanostruct. Mater.* **1** 27 (1992)
37. H Hahn, R S Averback *J. Appl. Phys.* **67** 1113 (1990)
38. G Skandan, H Hahn, J C Parker *Scr. Metall. Mater.* **25** 2389 (1991)
39. S Iwama, K Hayakawa, T Arizumi *J. Cryst. Growth* **56** 265 (1982)
40. M S El-Shall, W Slack, W Vann, D Kane, D Hanley *J. Phys. Chem.* **98** 3067 (1994)
41. Yu I Petrov, E A Shafranovsky, Yu F Krupyanskii, S V Essine *J. Appl. Phys.* **91** 352 (2002)
42. Yu A Bykovskii, V P Kozlenkov, Yu B Krasil'nikov, I N Nikolaev *Poverkhnost* (12) 69 (1992)
43. B H Kear, P R Strutt *Nanostruct. Mater.* **6** 227 (1995)
44. V N Troitskii, S V Gurov, V I Berestenko *Khim. Vys. Energ.* **13** 267 (1979) [e]
45. T N Miller *Izv. Akad. Nauk SSSR, Neorg. Mater.* **15** 557 (1979) [f]
46. T Ya Kosolapova, G N Makarenko, D P Zyatkevich *Zh. Vses. Khim. O-va im D I Mendeleeva* **24** 228 (1979) [g]
47. V F Petrunin, Yu G Andreev, T N Miller, Ya P Grabis *Poroshk. Metallurg.* (9) 90 (1987) [h]
48. I V Blinkov, A V Ivanov, I E Orekhov *Fiz. Khim. Obrab. Mater.* (2) 73 (1992)
49. K Kijima, H Nogushi, M Konishi *J. Mater. Sci.* **24** 2929 (1989)
50. F Thevenot *The Physics and Chemistry of Carbides, Nitrides and Borides* (Ed. R Freer) (Dordrecht: Kluwer Academic, 1990) p. 87
51. A I Gusev *Fizicheskaya Khimiya Nestekhiometricheskikh Tugoplavkikh Soedinenii* (Physical Chemistry of Non-stoichiometric Refractory Compounds) (Moscow: Nauka, 1991)
52. A V Lebedev, V A Moldaver, A S Kurlov, A A Rempel *Khimiya Tverdogo Tela i Funktsional'nye Materialy (Tezisy Dokladov Vserossiiskoi Konferentsii)* [Solid State Chemistry and Functional Materials (Abstracts of Reports of All-Russian Conference)] (Ekaterinburg: Urals Branch of the Russian Academy of Sciences, 2004) p. 237
53. A S Kurlov, S Z Nazarova, A A Rempel *Nanotekhnologiya i Fizika Funktsional'nykh Nanokristallicheskikh Materialov* (Nanotechnology and Physics of Functional Nanocrystalline Materials (Eds V V Ustinov, N I Noskova) (Ekaterinburg: Urals Branch of the Russian Academy of Sciences, 2005) Vol. 1, p. 59
54. J S Haggerty, W R Cannon *Laser-Induced Chemical Processes* (Ed. J I Steinfeld) (New York: Plenum, 1981)
55. N V Karlov, M A Kirichenko, B S Luk'yanchuk *Usp. Khim.* **62** 223 (1993) [*Russ. Chem. Rev.* **62** 203 (1993)]
56. E A Rohlfing, D M Cox, A Kaldor *J. Chem. Phys.* **81** 3322 (1984)
57. H W Kroto, J R Heath, S C O'Brien, R F Curl, R E Smalley *Nature (London)* **318** 162 (1985)
58. R F Curl, R E Smalley *Science* **241** 1017 (1988)
59. E Osawa *Kagaku (Kyoto)* **25** 854 (1970)
60. D A Bochvar, E G Gal'pern *Dokl. Akad. Nauk SSSR* **209** 610 (1973) [d]
61. L Hultman, S Stafstrom, Z Czigany, J Neidhardt, N Hellgren, I F Brunell, K Suenaga, C Colliex *Phys. Rev. Lett.* **87** 225503-1 (2001)
62. T Guo, M D Diener, Y Chai, M J Alford, R E Haufler, S M Mclure, T Ohno, J H Weaver, G E Scuseria, R E Smalley *Science* **257** 1661 (1992)
63. T Guo, R E Smalley, G E Scuseria *J. Chem. Phys.* **99** 352 (1993)
64. Z Lin, M B Hall *J. Am. Chem. Soc.* **115** 11165 (1993)
65. B C Guo, S Wei, J Purnell, S Buzza, A W Castleman *Science* **256** 515 (1992)
66. S Wei, B C Guo, J Purnell, S Buzza, A W Castleman *J. Phys. Chem.* **96** 4166 (1992)
67. J S Pilgrim, M A Duncan *J. Am. Chem. Soc.* **115** 4395 (1993)
68. B C Guo, A W Castleman *Advances in Metal and Semiconductor Clusters* (Ed. M Duncan) (Greenwich: JAI Press, 1994) Vol. 2, p. 137
69. A W Castleman *Annu. Rev. Phys. Chem.* **45** 685 (1994)
70. S Wei, B C Guo, H T Deng, K Kerns, J Purnell, S Buzza, A W Castleman *J. Am. Chem. Soc.* **116** 4475 (1994)
71. H van Swygenhoven, P Boni, F Paschoud, M Victoria, M Knauss *Nanostruct. Mater.* **6** 739 (1995)
72. R A Andrievskii *Usp. Khim.* **66** 57 (1997) [*Russ. Chem. Rev.* **66** 53 (1997)]
73. N Herron, Y Wang, M M Eddy, G D Stucky, D E Cox, K Moller, T Bein *J. Am. Chem. Soc.* **111** 530 (1989)
74. M Faraday *Philos. Trans. R. Soc. London* **147** 145 (1857)

75. N S Kozhevnikova, A A Rempel *Fizicheskaya Khimiya Vodnykh Rastvorov: Teoreticheskie Osnovy i Sintez Perspektivnykh Opticheskikh Materialov* (Physical Chemistry of Aqueous Solutions: Theoretical Foundations and Synthesis of Promising Optical Materials) (Ekaterinburg: Ural State Technical University-Ural Polytechnical University, 2006)
76. N S Belova, A A Rempel *Neorg. Mater.* **40** 7 (2004) [f]
77. N S Belova, A S Kurlov, A A Uritskaya, A A Rempel *Zh. Strukt. Khim. (Prilozhenie)* **45** 156 (2004) [i]
78. A A Rempel, N S Kozhevnikova, A J G Leenaers, S Van den Berghe *J. Cryst. Growth* **280** 300 (2006)
79. L Pasquini, A A Rempel, R Wurschum, K Reimann, M A Muller, B Fultz, H-E Schaefer *Phys. Rev. B* **63** 134114 (2001)
80. A A Rempel, N S Kozhevnikova, S Van den Berghe, W Van Renterghem *Phys. Status Solidi B* **242** (7) R61 (2005)
81. A A Rempel, N S Belova, A S Kurlov, A A Valeeva *The 7th International Conference on Nanostructured Materials 'NANO 2004', Wiesbaden, 2004* p. 307
82. N S Kozhevnikova, A A Rempel, F Hergert, S Jost, A Magerl *The 8th International Conference on Nanostructured Materials 'NANO 2006', Bangalore, 2006* p. 108
83. N S Kozhevnikova, A S Vorokh, A A Rempel *Biosovmestimye Nanostrukturnye Materialy i Pokrytiya Meditsinskogo Naznacheniya (Sbornik Nauchnykh Trudov Rossiiskoi Shkoly-konferentsii Molodykh Uchenykh i Prepodavatelei)* [Biocompatible Nanostructured Materials and Coatings for Medical Purposes (Proceedings of Russian School-conference of Young Scientists and Teachers)] (Belgorod: Institute of Solution Chemistry, Russian Academy of Sciences, 2006) p. 95
84. C B Murray, C R Kagan, M G Bawendi *Science* **270** 1335 (1995)
85. Q Lu, F Gao, D Zhao *Nanotechnology* **13** 741 (2002)
86. D V Talapin, E V Shevchenko, A Kornowski, N Gaponik, M Haase, A L Rogach, H Weller *Adv. Mater.* **13** 1868 (2001)
87. J H Warner, S Djouahra, R D Tilley *Nanotechnology* **17** 3035 (2006)
88. S Wong, V Kitaev, G A Ozin *J. Am. Chem. Soc.* **125** 15589 (2003)
89. A Chemseddine, T Moritz *Eur. J. Inorg. Chem.* 235 (1999)
90. I F Efremov *Periodicheskie Kolloidnye Struktury* (Periodical Colloid Structures) (Leningrad: Khimiya, 1971)
91. G Nikolis, I Prigogine *Self-organization in Nonequilibrium Systems* (New York: Wiley, 1977)
92. A Bleier, R Cannon *Better Ceramics Through Chemistry (MRS Symp. Proc.)* (Eds C J Brinker, D E Clark, D R Ulrich) (Pittsburg: Materials Research Society, 1986) p. 71
93. G Franz, G Schwier *Raw Materials for New Technologies* (Ed. M Kursten) (Stuttgardt: Nagele and Obermuller, 1990) p. 139
94. V M Chernov, V I Litvin, I F Mironyuk, V V Tsyrina *Neorg. Mater.* **29** 1019 (1993) [f]
95. Y Wang, N Herron *J. Phys. Chem.* **91** 257 (1987)
96. Y Wang, N Herron *J. Phys. Chem.* **92** 4988 (1988)
97. V N Bogomolov *Usp. Fiz. Nauk* **124** 171 (1978) [*Physics-Uspekhi* **21** 77 (1978)]
98. A R Kortan, R Hull, R L Opila, M G Bawendi, M L Steigerwald, P J Carrol, L E Brus *J. Am. Chem. Soc.* **112** 1327 (1990)
99. A Haesselbarth, A Eychmuller, R Eichberger, M Giersig, A Mews, H Weller *J. Phys. Chem.* **97** 5333 (1993)
100. P V Kamat, B Patrick *J. Phys. Chem.* **96** 6829 (1992)
101. I Bedja, P V Kamat *J. Phys. Chem.* **99** 9182 (1995)
102. G Schmid *Nanostruct. Mater.* **6** 15 (1995)
103. G Schmid, M Harms, J-O Malm, J-O Bovin, J van Ruitenbeck, H W Zandbergen, W T Fu *J. Am. Chem. Soc.* **115** 2046 (1993)
104. F Hatakeyama, Sh Kanzaki *J. Am. Ceram. Soc.* **73** 2107 (1990)
105. L E McCandlish, B H Kear, B K Kim *Nanostruct. Mater.* **1** 119 (1992)
106. L Wu, J Lin, B K Kim, B H Kear, L E McCandlish *Proceedings of the 13th International Plansee Seminar* Vol. 3 (Eds H Bildstein, R Eck) (Reutte: Metallwerk Plansee, 1993) p. 667
107. US P. 5352269; *Chem. Abstr.* **121** 306171a (1994)
108. Z Fang, J W Eason *Proceedings of the 13th International Plansee Seminar* Vol. 3 (Eds H Bildstein, R Eck) (Reutte: Metallwerk Plansee, 1993) p. 625
109. P Seegopaul, L E McCandlish *Adv. Powder Metall. Part. Mater.* **3** 13-3 (1995)
110. P Seegopaul, L E McCandlish, F M Shinneman *Int. J. Refract. Met. Hard Mater.* **15** 133 (1997)
111. S Hotchandani, P V Kamat *J. Phys. Chem.* **96** 6834 (1992)
112. I Bedjia, S Hotchandani, P V Kamat *J. Phys. Chem.* **97** 11064 (1993)
113. B O'Regan, M Gratzel, D Fitzmaurice *Chem. Phys. Lett.* **183** 89 (1991)
114. H Yoshiki, K Hashimoto, A Fujishima *J. Electrochem. Soc.* **142** 428 (1995)
115. L Kavan, T Stoto, M Gratzel, D Fitzmaurice, V Shklover *J. Phys. Chem.* **93** 9493 (1993)
116. K Yamada, T Y Chow, T Horihata, M Nagata *J. Non-Cryst. Solids* **100** 316 (1988)
117. H Natter, M Schmelzer, R Hempelmann *J. Mater. Res.* **13** 1186 (1998)
118. I D Morokhov, L I Trusov, V N Lapovok *Fizicheskie Yavleniya v Ul'tradispersnykh Sredakh* (Physical Effects in Ultradispersed Media) (Moscow: Energoatomizdat, 1984)
119. Yu I Petrov *Klastery i Malye Chastitsy* (Clusters and Small Particles) (Moscow: Nauka, 1986)
120. V N Krasil'nikov, O I Gyrdasova, G V Bazuev *Izv. Akad. Nauk, Ser. Fiz.* **70** 988 (2006) [c]
121. V N Krasil'nikov, A P Shtin, O I Gyrdasova, G P Shveikin *VI Nauchnaya Konferentsiya 'Khimiya Tverdogo Tela i Sovremennye Mikro- i Nanotekhnologii' (Tezisy Dokladov)* [The VIth Scientific Conference 'Solid State Chemistry and Modern Micro- and Nanotechnologies' (Abstracts of Reports)] (Kislovodsk, Stavropol': North Caucasus State Technological University, 2006) p. 70
122. N T Kuznetsov *Materials Science of Carbides, Nitrides and Borides* (Eds Y G Gogotsi, R A Andrievski) (Dordrecht: Kluwer Academic, 1999) p. 223
123. K E Gonsalves, K T Kembaiyan *Solid State Ionics* **32 – 33** 661 (1989)
124. M Peuckert, T Vaahs, M Bruck *Adv. Mater.* **2** 398 (1990)
125. M G Mirabelli, A T Lynch, L G Sheddon *Solid State Ionics* **32 – 33** 655 (1989)
126. T Wade, J Park, E G Garza, C B Ross, D M Smith, R M Crooks *J. Am. Chem. Soc.* **114** 9457 (1992)
127. R Riedel, A Kienzle, W Dreβler, L M Ruwisch, J Bill, F Aldinger *Nature (London)* **382** 796 (1996)
128. K J Reichle, K Reimann, W Sprengel, A A Rempel, A Muller, H-E Schaefer *Int. J. Mater. Res.* **97** 621 (2006)
129. P Yu Butyagin *Usp. Khim.* **63** 1031 (1994) [*Russ. Chem. Rev.* **63** 965 (1994)]
130. V V Boldyrev *Usp. Khim.* **75** 201 (2006) [*Russ. Chem. Rev.* **75** 177 (2006)]
131. N F Uvarov, V V Boldyrev *Usp. Khim.* **70** 307 (2001) [*Russ. Chem. Rev.* **70** 265 (2001)]
132. A R Yavari, P J Desre, T Benameur *Phys. Rev. Lett.* **68** 2235 (1992)
133. H-J Fecht *Nanostruct. Mater.* **6** 33 (1995)
134. P Yu Butyagin, A N Streletskii *Fiz. Tv. Tela* **47** 830 (2005) [a]
135. V V Zyryanov *Mekhanokhimicheskii Sintez v Neorganicheskoi Khimii* (Mechanochemical Synthesis in Inorganic Chemistry) (Ed. E G Avvakumov) (Novosibirsk: Nauka, 1991) p. 102
136. A A Popovich, V P Reva, V N Vasilenko, V A Popovich, O A Belous *Poroshk. Metallurg.* (2) 37 (1993) [h]
137. V Yu Davydkin, L I Trusov, P Yu Butyagin, V V Moskvin, I V Kolbanev, V I Novikov, S S Plotkin *Mekhanokhimicheskii Sintez v Neorganicheskoi Khimii* (Mechanochemical Synthesis in Inorganic Chemistry) (Ed. E G Avvakumov) (Novosibirsk: Nauka, 1991) p. 183
138. N Atsumi, K Yoshioka, T Yamasaki, Y Ogino *Funtai Oyobi Funmatsu Yakin* **40** 261 (1993)
139. A Teresiak, H Kubsch *Nanostruct. Mater.* **6** 671 (1995)

140. D Oleszak, H Matyja *Nanostruct. Mater.* **6** 425 (1995)
141. J S C Jang, C C Koch *J. Mater. Res.* **5** 498 (1990)
142. W H Hall *Proc. Phys. Soc., Sect. A, Pt. 11* **62** 741 (1949)
143. W H Hall, G K Williamson *Proc. Phys. Soc., Sect. B, Pt. 11* **64** 937 (1951)
144. G K Williamson, W H Hall *Acta Metall.* **1** 22 (1953)
145. M A Xueming, J I Gang *J. Alloys Compd.* **245** L30 (1996)
146. M S El-Eskandarany, M Omori, T Kamiyama, T J Konno, K Sumiyama, T Hirai, K Suzuki *Sci. Rep. Res. Inst. Tohoku Univ., Ser. A* **43** 181 (1997)
147. P S de Carli, J C Jamieson *Science* **133** 1821 (1961)
148. L F Trueb *J. Appl. Phys.* **42** 503 (1971)
149. A M Staver, N V Gubareva, A I Lyamkin, E A Petrov *Fiz. Goren. Vzryva* **20** 100 (1984) [j]
150. A I Lyamkin, E A Petrov, A P Ershov, G V Sakovich, A M Staver, V M Titov *Dokl. Akad. Nauk SSSR* **302** 611 (1988) [b]
151. I Yu Mal'kov, L I Filatov, V M Titov, B V Litvinov, A L Chuvilin, T S Teslenko *Fiz. Goren. Vzryva* **29** 131 (1993) [i]
152. A G Beloshapko, A A Bukaemskii, A M Staver *Fiz. Goren. Vzryva* **26** 93 (1990) [j]
153. A G Beloshapko, A A Bukaemskii, I G Kuz'min, A M Staver *Fiz. Goren. Vzryva* **29** 111 (1993) [j]
154. A G Merzhanov, S Yu Sharivker *Materials Science of Carbides, Nitrides and Borides* (Eds Y G Gogotsi, R A Andrievski) (Dordrecht: Kluwer Academic, 1999) p. 205
155. A G Merzhanov *Usp. Khim.* **72** 323 (2003) [*Russ. Chem. Rev.* **72** 289 (2003)]
156. H H Nersisyan, J H Lee, C W Won *J. Mater. Res.* **17** 2859 (2002)
157. H Gleiter *Deformation of Polycrystals: Mechanisms and Microstructures* (Eds N Hansen, A Horsewell, T Leffers, H Lilholt) (Roskilde, Denmark: Risø Natl. Laboratory, 1981) p. 15
158. R W Siegel, H Hahn *Current Trends in Physics of Materials* (Ed. M Yussouff) (Singapore: World Sci. Publ., 1987) p. 403
159. E N Yakovlev, G M Gryaznov, V I Serbin, V N Lapovok, L I Trusov, V Ya Ganelin, E V Kapitanov, N B Kukhar', V B Begoulev *Poverkhnost* (4) 138 (1983)
160. R A Andrievskii *Poroshkovoe Materialovedenie* (Powder Materials Science) (Moscow: Metallurgiya, 1991)
161. M D Matthews, A Pechenik *J. Am. Ceram. Soc.* **74** 1547 (1991)
162. D-J Chen, M J Mayo *Nanostruct. Mater.* **2** 469 (1992)
163. T Rabe, R Wasche *Nanostruct. Mater.* **6** 357 (1995)
164. V S Urbanovich *Nanostructured Materials. Science and Technology, Ser. 3 (NATO ASI Ser.)* Vol. 50 (Eds G M Chow, N I Noskova) (Dordrecht: Kluwer Academic, 1998) p. 405
165. R A Andrievskii, V S Urbanovich *Fizikokhimiya Ul'tradispersnykh Sistem (Sbornik Nauchnykh Trudov V Vserossiiskoi Konferentsii)* [Physical Chemistry of Ultradispersed Systems (Proceedings of Vth All-Russian Conference)] (Ekaterinburg: Urals Branch of the Russian Academy of Sciences, 2001) Vol. 2, p. 118
166. G V Ivanov, N A Yavorovskii, Yu A Kotov, V I Davydovich, G A Mel'nikova *Dokl. Akad. Nauk SSSR* **275** 873 (1984) [b]
167. V V Ivanov, S N Paranin, E A Gavrilin, A V Petrichenko, Yu A Kotov, S A Lebedev, S M Cheshnitskii *Sverkhprovodimost': Fiz., Khim., Tekh.* 1112 (1992)
168. V V Ivanov, S N Paranin, A N Vikhrev, A A Nozdrin *Materialovedenie* (5) 49 (1997)
169. V V Ivanov, Yu A Kotov, O M Samatov, R Bohme, H U Karow, G Schumacher *Nanostruct. Mater.* **6** 287 (1995)
170. V V Ivanov, A N Vikhrev, A A Nozdrin *Fiz. Khim. Obrab. Mater.* (3) 67 (1997)
171. R A Andrievskii, A N Vikhrev, V V Ivanov, R I Kuznetsov, N I Noskova, V A Sazonova *Fiz. Met. Metalloved.* **81** (1) 137 (1996) [k]
172. R A Andrievskii, O M Grebtsova, E P Domashneva, I A Kiyanskii, E N Kurkin, V E Perel'man, V I Sinitsyn, O D Torbova, V I Torbov *Dokl. Akad. Nauk* **331** 306 (1993) [b]
173. V V Ivanov, S N Paranin, A V Nikonov, V R Khrustov, S V Dobrov *Fiziko-khimiya Ul'tradispersnykh (Nano-) Sistem (Sbornik Nauchnykh Trudov VI Vserossiiskoi Konferentsii)* [Physical Chemistry of Ultradispersed (Nano-) Systems (Proceedings of the VIth All-Russian Conference)] (Moscow: Moscow Engineering Physics Institute, 2003) p. 194
174. O L Khasanov, E S Dvilis, Yu P Pokholkov, V M Sokolov *Perspektiv. Mater.* (3) 88 (1999)
175. O L Khasanov, V M Sokolov, E S Dvilis, Yu P Pokholkov *Perspektiv. Mater.* (1) 76 (2002)
176. Yu Bykov, A Eremeev, V Flyagin, V Kaurov, A Kuftin, A Luchinin, O Malygin, I Plotnikov, V Zapevalov *Br. Ceram. Trans.* **59** 133 (1995)
177. S Egorov, A Eremeev, A Sorokin, Yu Bykov, A Rachkovskii, A Poduretz *Nanoscience and Technology (Proccedings of the Xth APAM Topical Seminar), Novosibirsk, 2003* p. 162
178. S Herth, H Rosner, A A Rempel, H-E Schaefer, R Wurschum *Z. Metallkd.* **94** 1073 (2003)
179. H Hoffmann *Thin Solid Films* **58** 223 (1979)
180. Y Yoshizawa, S Oguma, K Yamauchi *J. Appl. Phys.* **64** 6044 (1988)
181. N I Noskova, N F Vil'danova, A P Potapov, A A Glazer *Fiz. Met. Metalloved.* **73** (2) 102 (1992) [j]
182. A Inoue, H M Kimura, K Sasamori, T Masumoto *Mater. Trans., JIM* **35** 85 (1994)
183. N A Smirnova, V I Levit, V P Pilyugin, R I Kuznetsov, M V Degtyarev *Fiz. Met. Metalloved.* **62** 566 (1986) [k]
184. R Z Valiev, N A Krasilnikov, N K Tsenev *Mater. Sci. Eng., A* **137** 35 (1991)
185. R Z Valiev, A V Korznikov, R R Mulyukov *Fiz. Met. Metalloved.* **73** (4) 70 (1992) [k]
186. V M Segal *Mater. Sci. Eng., A* **197** 157 (1995)
187. V M Segal, Author's abstract of Doctoral Thesis in Technical Sciences, Physical Technical Institute, Academy of Sciences of the Bel.SSR, Minsk, 1974
188. V M Segal, V I Reznikov, F E Drobyshevskii, V I Kopylov *Izv. Akad. Nauk SSSR, Ser. Metally* (1) 115 (1981)
189. V M Segal, V I Reznikov, V I Kopylov, D A Pavlik, V F Malyshev *Protsessy Plasticheskogo Strukturoobrazovaniya Metallov* (Processes of Plastic Structurisation of Metals) (Minsk: Nauka i Tekhnika, 1994)
190. R Z Valiev, A V Korznikov, R R Mulyukov *Mater. Sci. Eng., A* **168** 141 (1993)
191. N A Akhmadeev, R Z Valiev, V I Kopylov, R R Mulyukov *Metally* (5) 96 (1992)
192. A A Rempel, A I Gusev, S Z Nazarova, R R Mulyukov *Dokl. Akad. Nauk* **347** 750 (1996) [b]
193. A Cziraki, I Geracs, E Toth-Kadar, I Bakonyi *Nanostruct. Mater.* **6** 547 (1995)
194. A A Rempel, A I Gusev, R R Mulyukov, N M Amirkhanov *Metallofiz. Noveish. Tekhnol.* (7) 14 (1996)
195. A A Rempel, A I Gusev *Phys. Status Solidi B* **196** 251 (1996)
196. A A Rempel, A I Gusev, R R Mulyukov, N M Amirkhanov *Nanostruct. Mater.* **7** 667 (1996)
197. A A Rempel, A I Gusev, S Z Nazarova, R R Mulyukov *Dokl. Akad. Nauk* **345** 330 (1995) [b]
198. R Z Valiev, R R Mulyukov, V V Ovchinnikov, V A Shabashov *Scr. Metall. Mater.* **25** 2717 (1991)
199. R Z Valiev, Ya D Vishnyakov, R R Mulyukov, G S Fainstein *Phys. Status Solidi A* **117** 549 (1990)
200. Kh Ya Mulyukov, G F Korznikova, R Z Valiev *Phys. Status Solidi A* **125** 609 (1991)
201. R Z Abdulov, R Z Valiev, N A Krasilnikov *J. Mater. Sci. Lett.* **9** 1445 (1990)
202. R M Galeev, O R Valiakhmetov, G A Salishchev *Izv. Akad. Nauk SSSR, Ser. Metally* (4) 97 (1990)
203. O R Valiakhmetov, R M Galeev, G A Salishchev *Fiz. Met. Metalloved.* **70** (10) 204 (1990) [k]

204. A A Rempel, A I Gusev, R R Mulyukov *Khimiya Tverdogo Tela i Novye Materialy* (Solid State Chemistry and New Materials) (Ekaterinburg: Institute of Solid State Chemistry Urals Branch of the Russian Academy of Sciences, 1996) Vol. 1, p. 244
205. A A Rempel, A I Gusev, R R Mulyukov *Ul'tradispersnye Poroshki, Materialy i Nanostruktury* (Ultradispersed Powders, Materials and Nanostructures) (Ed. V E Red'kin) (Krasnoyarsk: Krasnoyarsk State Technical University, 1996) p. 131
206. A A Valeeva, B A Gizhevskii, V P Pilyugin, A A Rempel *Fiz. Met. Metalloved.* **99** (1) 62 (2005) [k]
207. M M Martynyuk *Zh. Tekhn. Fiz.* **44** 1262 (1974) [l]
208. Yu A Kotov, N A Yavorskii *Fiz. Khim. Obrab. Mater.* (4) 24 (1978)
209. V A Burtsev, N V Kalinin, A V Luchinskii *Elektricheskii Vzryv Provodnikov i ego Primenenie v Elektrofizicheskikh Ustanovkakh* (Electrical Explosion of Conductors and Its Application in Elecrophysical Facilities) (Moscow: Energoatomizdat, 1990)
210. A P Il'in, O B Nazarenko, D V Tikhonov *Ul'tradispersnye Poroshki, Nanostruktury, Materialy (Trudy Vtoroi Mezhregional'noi Konferentsii)* [Ultradispersed Powders, Nanostructures and Materials (Proceedings of the Second International Conference)] (Krasnoyarsk: Krasnoyarsk State Technical University, 1999) p. 31
211. A P Il'in *Fiz. Khim. Obrab. Mater.* (3) 94 (1994)
212. A P Il'in *Fiz. Khim. Obrab. Mater.* (4) 93 (1997)
213. A I Gusev, A A Rempel *Nestekhiometriya, Besporyadok i Poryadok v Tverdom Tele* (Non-stoichiometry, Disorder and Order in Solids) (Ekaterinburg: Ural Branch of the Russian Academy of Science, 2001)
214. A I Gusev, A A Rempel, A J Magerl *Disorder and Order in Strongly Nonstoichiometric Compounds: Transition Metal Carbides, Nitrides and Oxides* (Berlin, Heidelberg, New York: Springer, 2001)
215. A I Gusev, A A Rempel *Phys. Status Solidi A* **163** 273 (1997)
216. A I Gusev *Usp. Fiz. Nauk* **170** 3 (2000) [*Physics-Uspekhi* **43** 1 (2000)]
217. A I Gusev, A A Rempel *Strukturnye Fazovye Perekhody v Nestekhiometricheskikh Soedineniyakh* (Structural Phase Transitions in Non-stoichiometric Compounds) (Moscow: Nauka, 1988)
218. A A Rempel *Effekty Uporyadocheniya v Nestekhiometricheskikh Soedineniyakh Vnedreniya* (Ordering Effects in Non-stoichiometric Interstitial Compounds) (Ekaterinburg: Nauka, 1992)
219. A A Rempel *Usp. Fiz. Nauk* **166** 33 (1996) [*Physics-Uspekhi* **39** 31 (1996)]
220. A I Gusev, A A Rempel *Phys. Status Solidi A* **135** 15 (1993)
221. T Athanassiadis, N Lorenzelli, C H de Novion *Ann. Chim. (Paris)* **12** 129 (1987)
222. A A Rempel, A I Gusev *Pis'ma Zh. Eksp. Teor. Fiz.* **69** 436 (1999) [m]
223. V N Lipatnikov, W Lengauer, P Ettmayer, E Keil, G Groboth, E Kny *J. Alloys Compd.* **261** 192 (1997)
224. D Rafaja, W Lengauer, P Ettmayer, V N Lipatnikov *J. Alloys Compd.* **269** 60 (1998)
225. A A Rempel, A I Gusev, O V Makarova, S Z Nazarova *Perspekt. Mater.* (6) 9 (1999)
226. A I Gusev, A A Tulin, V N Lipatnikov, A A Rempel *Zh. Obshch. Khim.* **72** 1067 (2002) [n]
227. R Würschum, H-E Schaefer *Nanomaterials: Synthesis, Properties and Applications* (Eds A S.Edelstein, R C Cammarata) (Bristol: Institute of Physics Publ., 1996) p. 277
228. A A Rempel, W Sprengel, K Blaurock, K J Reichle, J Major, H-E Schaefer *Phys. Rev. Lett.* **89** 185501 (2002)
229. A A Rempel, M Foster, G-E Shefer *Dokl. Akad. Nauk* **326** 91 (1992) [b]
230. A A Rempel, L V Zueva, V N Lipatnikov, H-E Schaefer *Phys. Status Solidi A* **169** R9 (1998)
231. A I Gusev *Zh. Fiz. Khim.* **74** 600 (2000) [o]
232. V N Belomestnykh, E P Tesleva *Fiziko-khimiya Ul'tradispersnykh (Nano-) Sistem (Sbornik Nauchnykh Trudov VI Vserossiiskoi Konferentsii)* [Physical Chemistry of Ultradispersed (Nano-) Systems (Proceedings of the VIth All-Russian Conference)] (Moscow: Moscow Eengineering Physics Institute, 2003) p. 200
233. O B Naimark *Fiz. Met. Metalloved.* **84** (4) 5 (1997) [k]
234. E Kroner *Lecture Notes in Physics* (Eds E Kroner, K Kinchgassner) (Heidelberg: Springer, 1986) p. 281
235. A Kadiå, D G B Edelen *A Gauge Theory of Dislocations and Disclinations* (Berlin: Springer, 1983)
236. T L Makarova, B Sundqvist, R Höhne, P Esquinazi, Ya Kopelevich, P Schraff, V A Davydov, L S Kashevarova, A V Rakhmanina *Nature (London)* **413** 716 (2001)
237. K Sohlberg, R E Tuzun, B Sumpter, D W Noid *Nanotechnology* **8** 103 (1997)
238. L Delzeit, C V Nguyen, R M Stevens, J Han, M Meyyappan *Nanotechnology* **13** 280 (2002)
239. M Menon, D Srivastava *Phys. Rev. Lett.* **79** 4453 (1997)
240. J Li, C Papadopoulos, J Xu *Nature (London)* **402** 253 (1999)
241. C Papadopoulos, A Rakitin, J Li, A S Vedeneev, J M Xu *Phys. Rev. Lett.* **85** 3476 (2000)
242. B Q Wei, R Vajtai, Y Jung, J Ward, Y Zhang, G Ramanath, P M Ajayan *Nature (London)* **416** 495 (2002)
243. P Kral, D Tomanek *Phys. Rev. Lett.* **82** 5373 (1999)
244. E G Rakov *Usp. Khim.* **70** 934 (2001) [*Russ. Chem. Rev.* **70** 827 (2001)]
245. A L Ivanovskii *Usp. Khim.* **71** 203 (2002) [*Russ. Chem. Rev.* **71** 175 (2002)]
246. V V Pokropivnyi *Poroshk. Metall.* (3–4) 13 (2002) [h]
247. M Che, C O Bennet *Adv. Catal.* **36** 55 (1989)
248. V I Bukhtiyarov, M G Slin'ko *Usp. Khim.* **70** 167 (2001) [*Russ. Chem. Rev.* **70** 147 (2001)]
249. V Ponec *Adv. Catal.* **32** 149 (1983)
250. Z Karpinski *Adv. Catal.* **37** 45 (1990)
251. A D Pomogailo *Usp. Khim.* **69** 60 (2000) [*Russ. Chem. Rev.* **69** 53 (200)]
252. A D Pomogailo, A S Rozenberg, I E Uflyand *Nanochastitsy Metallov v Polimerakh* (Nanoparticles of Metals in Polymers) (Moscow: Khimiya, 2000)
253. J S Kilby *Usp. Fiz. Nauk* **172** 1102 (2002) [Nobel Lectures, Physics 1996-2000 (Ed. G. Ekspong) (Singapore: World Sci. Publ., 2002)]
254. D L Klein, R Roth, A K L Lim, A P Alivisatos, P L McEuen *Nature (London)* **389** 699 (1997)
255. A Erbe, C Weiss, W Zwerger, R H Blick *Phys. Rev. Lett.* **87** 096106 (2001)
256. H Kroemer *Usp. Fiz. Nauk* **172** 1091 (2002) [Nobel Lectures, Physics 1996-2000 (Ed. G. Ekspong) (Singapore: World Sci. Publ., 2002)]
257. R Dingle, W Wiegmann, C H Henry *Phys. Rev. Lett.* **33** 827 (1974)
258. Zh I Alferov *Usp. Fiz. Nauk* **172** 1072 (2002) [Nobel Lectures, Physics 1996-2000 (Ed. G. Ekspong) (Singapore: World Sci. Publ., 2002)]
259. A P Alivisatos *Science* **271** 933 (1996)
260. K Morgenstern *Phys. J.* **1** 95 (2002)
261. Yu P Pershin, E N Zubarev, V V Kondratenko, O V Pol'tseva, A G Ponomarenko, V A Sevryukova, Ya Verkhoeven *Metallofiz. Noveish. Tekhnol.* **24** 795 (2002)
262. J J Hauser, H C Theuerer, N R Werthamer *Phys. Rev.* **142** 118 (1966)
263. B Y Jin, J B Ketterson *Adv. Phys.* **38** 189 (1989)
264. A I Buzdin, A V Vedyayev, N V Ryshanova *Europhys. Lett.* **48** 686 (1999)
265. L R Tagirov *Phys. Rev. Lett.* **83** 2058 (1999)
266. Yu A Izyumov, Yu N Proshin, M G Khusainov *Usp. Fiz. Nauk* **172** 113 (2002) [*Physics-Uspekhi* **45** 109 (2002)]
267. A S Borukhovich *Usp. Fiz. Nauk* **169** 737 (1999) [*Physics-Uspekhi* **42** 653 (1999)]

268. O L Khasanov, E S Dvilis, V M Sokolov, Yu P Pokholkov *Fiziko-khimiya Ul'tradispersnykh (Nano-) Sistem (Sbornik Nauchnykh Trudov VI Vserossiiskoi Konferentsii)* [Physical Chemistry of Ultradispersed (Nano-) Systems (Proceedings of the VIth All-Russian Conference)] (Moscow: Moscow Engineering Physics Institute, 2003) p. 180
269. Yu V Kolen'ko, P E Meskin, V A Mukhanov, B R Churagulov, S V Balakhonov *Zh. Neorg. Khim* **50** 1941 (2005) [p]
270. Y V Kolen'ko, K A Kovnir, A I Gavrilov, A V Garshev, J Frantti, O I Lebedev, B R Churagulov, G Van Tendeloo, M Yoshimura *J. Phys. Chem. B* **110** 4030 (2006)
271. J H Fendler *Membrane-mimetic Approach to Advance Materials*. (Berlin, Heidelberg, New York: Springer, 1994)

[a] — *Phys. Solid State (Engl. Transl.)*
[b] — *Dokl. Phys. (Engl. Transl.)*
[c] — *Bull. Russ. Acad. Sci., Phys. (Engl. Transl.)*
[d] — *Dokl. Chem. (Engl. Transl.)*
[e] — *High Energ. Chem. (Engl. Transl.)*
[f] — *Inorg. Mater. (Engl. Transl.)*
[g] — *Mendeleev Chem. J. (Engl. Transl.)*
[h] — *Powder Metall. Met. Ceram. (Engl. Transl.)*
[i] — *J. Struct. Chem. (Engl. Transl.)*
[j] — *Comp. Explos. Shock Waves (Engl. Transl.)*
[k] — *Phys. Met. Metallogr. (Engl. Transl.)*
[l] — *Techn. Phys. (Engl. Transl.)*
[m] — *J. Exp. Theor. Phys. Lett. (Engl. Transl.)*
[n] — *Russ. J. Gen. Chem. (Engl. Transl.)*
[o] — *Russ. J. Phys. Chem. (Engl. Transl.)*
[p] — *Russ. J. Inorg. Chem. (Engl. Transl.)*